HU-EP-24/16-RTG

Post-Minkowskian Theory Meets the Spinning Effective-One-Body Approach for Bound-Orbit Waveforms

Alessandra Buonanno,[1,2] Gustav Mogull,[1,3] Raj Patil,[1,3] and Lorenzo Pompili[1]

[1]*Max Planck Institute for Gravitational Physics (Albert Einstein Institute), Am Mühlenberg 1, 14476 Potsdam, Germany*
[2]*Department of Physics, University of Maryland, College Park, MD 20742, USA*
[3]*Institut für Physik und IRIS Adlershof, Humboldt Universität zu Berlin, Zum Großen Windkanal 2, 12489 Berlin, Germany*

Driven by advances in scattering amplitudes and worldline-based methods, recent years have seen significant progress in our ability to calculate gravitational two-body scattering observables. These observables effectively encapsulate the gravitational two-body problem in the weak-field and high-velocity regime (post-Minkowskian, PM), with applications to the bound two-body problem and gravitational-wave modeling. We leverage PM data to construct a complete inspiral-merger-ringdown waveform model for non-precessing spinning black holes within the effective-one-body (EOB) formalism: `SEOBNR-PM`. This model is closely based on the highly successful `SEOBNRv5` model, used by the LIGO-Virgo-KAGRA Collaboration, with its key new feature being an EOB Hamiltonian derived by matching the two-body scattering angle in a perturbative PM expansion. The model performs remarkably well, showing a median mismatch against 441 numerical-relativity (NR) simulations that is somewhat lower than a similarly calibrated version of `SEOBNRv5`. Comparisons of the binding energy with NR also demonstrate better agreement than `SEOBNRv5`, despite the latter containing additional calibration to NR simulations.

arXiv:2405.19181v1 [gr-qc] 29 May 2024

Introduction – Since the initial detection of a gravitational wave (GW) from a binary–black-hole (BBH) merger [1], the LIGO-Virgo-KAGRA (LVK) Collaboration [2–4] and independent analyses have identified about 100 mergers of compact binaries [5–10]. These observations have begun to reveal the distributions of BH-masses and spins [11], improved constraints on the neutron-star (NS) equation of state [12], obtained independent measurements of the Hubble-Lemaître parameter [13, 14], and validated General Relativity (GR) [15–17].

Enhancements in the sensitivity of current GW detectors, coupled with the development of next-generation (XG) observatories like the Einstein Telescope and Cosmic Explorer [18–20], as well as future space-based detectors such as LISA [21], TianQin [22] or Taiji [23], are poised to dramatically increase the number of detectable GW sources. These advancements will enable observations with a signal-to-noise ratio up to two orders of magnitude higher than what is currently achievable [24], necessitating a commensurate improvement in the accuracy of waveform models. Recent research [25] has demonstrated that even state-of-the-art waveform models, designed for quasi-circular, spin-precessing BBHs, exhibit systematic biases when applied to future LVK runs and XG detectors. This bias becomes pronounced, especially for high-spin rates and significant asymmetries in spins and masses. Addressing the challenge of waveform accuracy is essential to realizing the full scientific potential of future runs and detectors [24, 26–29], and avoiding false claims of GR violations [30, 31].

Waveform models for compact binaries are crafted by synergistically combining analytical and numerical relativity (NR) results. NR tackles the formidable task of solving Einstein's equations on supercomputers [32–34], a process notorious for its time-intensive nature. On the other hand, perturbative methods are used to obtain approximate solutions to the Einstein's equations, offering analytic formulas that are swift to evaluate. Three primary perturbative approaches have been developed: (i) post-Newtonian (PN) theory [35–50] applicable in the weak-field and small-velocity limit, post-Minkowskian (PM) theory [51–60] in the weak-field regime, and the gravitational-self force (GSF) formalism [61–74] for the small mass-ratio limit. These analytical results are then synthesized in the effective-one-body (EOB) approach [75–79], which efficiently resums the perturbative calculations for the inspiral while retaining known non-perturbative results for BHs, achieving high accuracy for current observing runs via calibration to NR [80–94].

Thus far, the EOB waveform models utilized by the LVK Collaboration [95] have primarily relied on resummations of the PN expansion, with the exception of Refs. [94, 96], which included second-order GSF results [73] for the gravitational modes and radiation-reaction force. Given recent advancements in PM [97–111] and GSF [73, 74], there is now significant interest in exploring and developing waveform models that combine information from various perturbative methods in innovative ways. The aim is to address the waveform-accuracy challenge. In this regard, the PM approach is particularly interesting since an $(n+1)$ PM-order Hamiltonian includes all information up to the nPN order, and additional weak-field/high-velocity information from infinitely higher PN orders, making it suitable for systems with high velocities or large eccentricities at fixed periastron distances [112]. Using sophisticated quantum-field-theory–based methods, tremendous progress has been made on the precision PM-frontier using both scattering amplitudes [113–115] and worldlines [116–119]. This progress is largely due to a blend of a clever and efficient organization of perturbative calculations and formal mathematical developments in understanding the

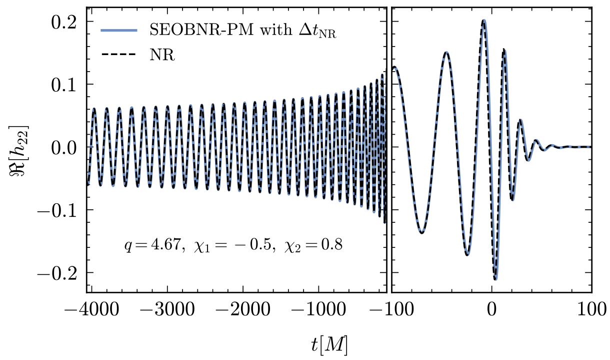

FIG. 1. An `SEOBNR-PM` inspiral-merger-ringdown waveform generated using the `pySEOBNR` code [150], compared against the NR simulation `SXS:BBH:1445`, after a low-frequency alignment by a time and phase shift. The time $t = 0$ corresponds to the peak of the $(2, 2)$ mode of the NR waveform.

properties of multi-loop integrals [120–126]. These developments were primarily driven over the last several decades to address precision-collider physics. Furthermore, several sophisticated techniques, such as generalized unitarity [127, 128], double copy [129–132], supersymmetry [110] and massive higher spins [133–140] have also been used to further enhance these computations

In this paper, leveraging on Refs. [93, 141, 142], we present the first PM-informed spinning EOB waveform model: `SEOBNR-PM`, encompassing the inspiral, as well as, the merger and ringdown phases. This model incorporates the most recent findings from PM theory into the EOB Hamiltonian, and it is mildly calibrated to NR waveforms. The `SEOB-PM` Hamiltonian (so-named as it does not include an NR calibration term) includes the non-spinning (conservative) 4PM [114, 116] and spinning 5PM terms [118, 135, 143–148], alongside the known non-spinning 4PN [41–45] contributions, which also corrects the tails from unbound to bound orbits up to that order [149]. Our PM counting is a physical one, with spin orders contributing in addition to loop orders (see Table II in Ref. [142]). We construct our `SEOBNR-PM` model within the `pySEOBNR` code [150], which was recently built to make the development of `SEOBNR` models, including the calibration to NR waveforms, highly efficient. As an example, we show in Fig. 1 the agreement between the (mildly) calibrated `SEOBNR-PM` and NR for a spinning BBH coalescence.

The EOB framework for waveforms – We use geometric units $G = 1 = c$, and set $M = m_1 + m_2$ and $\nu = m_1 m_2/M^2$, where m_1 and m_2 are the BH's masses. In the EOB formalism, the binary's conservative dynamics is described by the EOB Hamiltonian $H_{\rm EOB} = M\sqrt{1 + 2\nu(H_{\rm eff}/\mu - 1)}$, where $H_{\rm eff}$ is the Hamiltonian of an effective test-body of mass $\mu = \nu M$ moving in the (deformed) Kerr spacetime, being $0 \le \nu \le 1/4$ the deformation parameter. We also introduce the mass ratio $q = m_1/m_2 > 1$. We limit to nonprecessing spins (i.e., aligned spins) and introduce the spin lengths $a_i = m_i\chi_i$, with $a_\pm = M\chi_\pm = a_1 \pm a_2$.

In the center-of-masss frame, the inspiral-plunge dynamics, for aligned-spin BHs, is computed from the EOB equations of motion [76, 83]:

$$\dot r = \frac{\partial H_{\rm EOB}}{\partial p_r}\,, \qquad \dot p_r = -\frac{\partial H_{\rm EOB}}{\partial r} + \frac{p_r}{p_\phi}\mathcal{F}_\phi\,, \tag{1a}$$

$$\dot \phi = \frac{\partial H_{\rm EOB}}{\partial p_\phi}\,, \qquad \dot p_\phi = \mathcal{F}_\phi\,, \tag{1b}$$

where (r,ϕ,p_r,p_ϕ) are the polar-coordinates canonical variables. (The construction of $H_{\rm eff}$ will be described in the next section.) Employing results from the `SEOBNRv5` model [93, 141], the radiation-reaction force $(\mathcal{F}_\phi)$ is computed by summing over the PN GW modes (augmented with GSF information [96]) in a factorized form [82, 93, 151–153], which are used to obtain the inspiral-plunge modes after enhancing them by non-quasi-circular corrections [86, 87, 93, 154] during the plunge.

For the merger-ringdown part of the EOB waveform, we use instead a phenomenological ansatz [87, 93, 155, 156], informed by NR and BH perturbation theory, as realized in the `SEOBNRv5` model [93]. The start of the merger-ringdown waveform is enforced to be at the peak of the $(2, 2)$-mode amplitude. The gravitational polarizations can be written as $h_+ - ih_\times = \sum_{\ell,m} {}_{-2}Y_{\ell m}(\varphi,\iota)h_{\ell m}(t)$, where ${}_{-2}Y_{\ell m}(\varphi,\iota)$ are the -2 spin-weighted spherical harmonics, with φ and ι being the azimuthal and polar angles to the observer, in the source frame. In the EOB approach, the inspiral-merger-ringdown (ℓ, m) modes are given by

$$h_{\ell m} = \begin{cases} h_{\ell m}^{\rm insp-plunge}, & t < t_{\rm peak}^{22}\,, \\ h_{\ell m}^{\rm merg-RD}, & t > t_{\rm peak}^{22}\,. \end{cases} \tag{2}$$

where $t_{\rm peak}^{22}$ is the time at which the (2,2) mode has a peak, generally associated to the merger time. Such a time is suitably chosen to agree with the corresponding time in NR waveforms (see below).

PM-informed EOB Hamiltonian – We employ an effective Hamiltonian similar to that recently introduced in the `SEOB-PM` scattering model [142]:

$$H_{\rm eff} = \frac{M p_\phi (g_{a_+} a_+ + g_{a_-}\delta a_-)}{r^3 + a_+^2(r + 2M)} + \sqrt{A\left(\mu^2 + \frac{p_\phi^2}{r^2} + (1 + B_{\rm np}^{\rm Kerr})p_r^2 + B_{\rm npa}^{\rm Kerr}\frac{p_\phi^2 a_+^2}{r^2}\right)}\,, \tag{3}$$

where $\delta = (m_1 - m_2)/M$, while $B_{\rm np}^{\rm Kerr} = \chi_+^2 u^2 - 2u$ and $B_{\rm npa}^{\rm Kerr} = -(1 + 2u)/[r^2 + a_+^2(1 + 2u)]$, where $u = M/r$ is the dimensionless PM counting parameter. In the probe limit $\nu \to 0$, $H_{\rm eff}$ reduces to the Hamiltonian of a probe μ moving under the influence of a Kerr BH with mass M and directed spin length a_+. This Hamiltonian is determined by computing the scattering angle and matching it to established PM results, but here we use only the conservative part of the angle containing terms with even powers in the center-of-mass momentum $p_\infty = \mu\sqrt{\gamma^2-1}$, where $\gamma = E_{\rm eff}/\mu > 1$ for scattering trajectories.

Following Ref. [142], the ν-corrections with respect to the probe limit are built into the A-potential and the gyro-gravitomagnetic factors as $A = (1-2u+\chi_+^2u^2+\Delta A)/[1+\chi_+^2u^2(2u+1)]$ and $g_{a_\pm} = \Delta g_{a_\pm}/u^2$. These respectively carry the even- and odd-in-spin corrections, and are PM-expanded up to a physical 5PM (u^5) order (see Table II in Ref. [142]):

$$\Delta A = \sum_{n=2}^{5} u^n \Delta A^{(n)} + \Delta A^{\rm 4PN}\,, \quad \Delta g_{a_\pm} = \sum_{n=2}^{5} u^n \Delta g_{a_\pm}^{(n)}\,. \tag{4}$$

The γ-dependent coefficients $\Delta A^{(n)}$ and $\Delta g_{a_\pm}^{(n)}$ are series expanded in even powers of the spins, up to a highest quartic order at 5PM. We lack an analytic 5PM term only in the non-spinning case, where the complete result is not currently known (see Ref. [157] for the recently derived 1GSF conservative contribution). Technically, as $\gamma = E_{\rm eff}/\mu \equiv H_{\rm eff}/\mu$, the Hamiltonian (3) is self-dependent. To produce an expression depending only on the canonical variables (r,p_r,p_ϕ), we interpret $\gamma = H_{\rm Kerr}/\mu$ within these deformations, plus whatever corrections are required in order to ensure the full Hamiltonian $H_{\rm EOB}$ is correct up to the desired PM order. This procedure was used previously in the non-spinning case [112, 158, 159], and is fully described in the Supplemental Material.

An important subtlety within our Hamiltonian is the presence of non-local-in-time contributions (tails). These imply a dependence on the full past history of the binary, and thus distinguish between elliptic and hyperbolic (scattering) trajectories. In the scattering Hamiltonian presented in Ref. [142], tails are signaled by factors of $\log(\gamma^2-1)$, which develops an imaginary part when $\gamma < 1$ for bound orbits. To produce a real Hamiltonian, we therefore replace $\log(\gamma^2-1) \to \log(u)$ (see Supplemental Material for details). We also include the 4PN non-spinning bound-orbit correction $\Delta A^{\rm 4PN}$ in Eq. (A2):

$$\Delta A^{\rm 4PN} = u^4(\gamma^2-1)c_1 + u^5(c_2 + c_3\log u)\,, \tag{5}$$

ensuring the correct bound-orbit dynamics at 4PN order in the non-spinning case (the numerical coefficients c_i are provided in the Supplemental Material). We verify our complete EOB Hamiltonian up to 4.5PN order [41, 160–163] by finding a suitable canonical transformation to its PN-expanded counterpart [164]. The non-spinning component is determined only up to quadratic order in eccentricity (p_r^2) in the tail integral, as higher powers in eccentricity appear at lower-PM orders. Thus, we ensured that the 1PM–3PM (tail-free) non-spinning dynamics are unmodified by the presence of the 4PN correction (5) [165].

Finally, let us comment on the appearance of special functions in $H_{\rm eff}$. Starting at 3PM order we encounter the combination $\text{arccosh}(\gamma)/\sqrt{\gamma^2-1}$. As $\text{arccosh}(\gamma)$ and $\sqrt{1-\gamma^2}$ are both imaginary-valued when $\gamma < 1$, we find it convenient to replace this combination by $\arccos(\gamma)/\sqrt{1-\gamma^2}$, which has the same small-velocity expansion for scattering kinematics. At 4PM order we then encounter logarithms, dilogarithms (Li_2) and elliptic functions (K/E) of the first and second kind, all evaluated as functions of γ. In this case, we also find it convenient to introduce the inverse tangent integral $\text{Ti}_2(x) := \int_0^x (\mathrm{d}t/t)\arctan t$, analogously to what is done above. Fast numerical routines exist for evaluating all of these functions in Cython [167], and this leads to an efficient numerical evaluation within `pySEOBNR` [150].

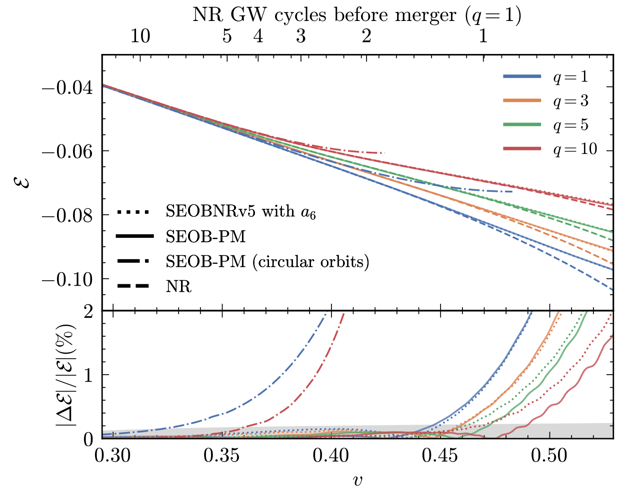

FIG. 2. Non-spinning binding energy as a function of the (quasi-circular) velocity $v = (M\dot\phi)^{2/3}$, for the (calibrated) `SEOBNRv5` with a_6 and (uncalibrated) `SEOB-PM` Hamiltonians (both along a circular orbit [112, 159] and inspiral) across different mass ratios $q = m_1/m_2$. The shaded region is an estimate of the NR uncertainty [166]. The lower panel shows the fractional difference.

Comparing `SEOB-PM` and NR binding energies during the inspiral– In EOB models one has access to the binary's dynamics, which enables testing their accuracy by comparing (gauge-invariant) dynamical quantities such as the binding energy [112, 166, 168–170] and periastron advance [171, 172]. As `SEOBNR-PM`'s essential new feature is its PM-informed `SEOB-PM` Hamiltonian, the binding energy is a particularly relevant quantity to compare with NR data. Previous comparisons in the non-spinning case [112, 159] have focused on the binding energy computed for circular orbits (i.e., ignoring radiation-reaction effects), although Ref. [159] investigated the effect of neglecting dissipation (see Fig. 6 therein). We instead compute the (dimensionless) binding energy by evaluating $\mathcal{E} = (H_{\rm EOB} - M)/\mu$ along the inspiraling dynamics, and compare with NR–binding-energy data from Ref. [166]. Fig. 2 shows the EOB and NR non-spinning binding energies as a function of the (quasi-circular) velocity parameter $v = (M\dot\phi)^{1/3}$, for `SEOBNRv5` with a_6 and `SEOB-PM` for circular orbits and along an inspiral. We stress that for the former, a 5PN-unknown parameter (a_6) in the A-potential has been calibrated against 18

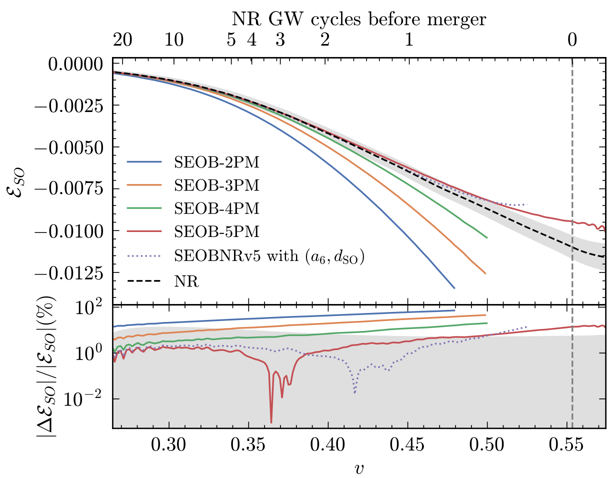

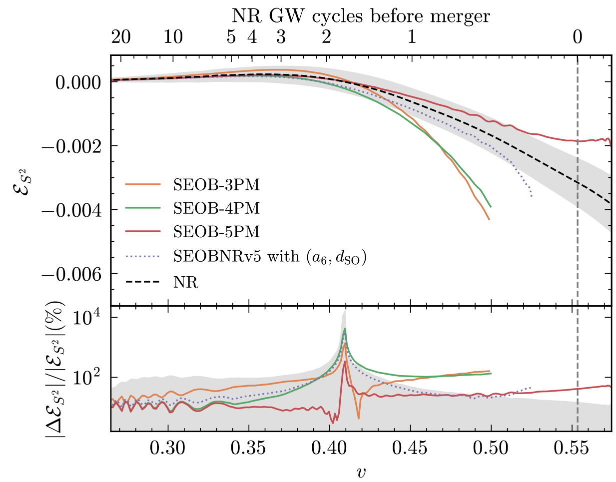

FIG. 3. Spin-orbit (left panel) and spin-squared (right panel) contributions to the binding energy, for an equal-mass BBH, as a function of the (quasi-circular) velocity $v = (M\dot{\phi})^{2/3}$, for the (calibrated) `SEOBNRv5` with (a_6,$d_{\rm SO}$) and (uncalibrated) `SEOB-PM` Hamiltonians at different PM orders. The vertical line represents the merger of the NR configuration (the one at the lowest velocity among those used), with the number of GW cycles (top axis) referring to the same simulation. The shaded regions are estimates of the NR uncertainty [166]. The lower panel shows the absolute value of the fractional difference. The feature in the lower-right panel around $v \sim 0.4$ is due to a zero-crossing.

non-spinning simulations (see below). Both models show excellent agreement with NR during most of the inspiral, with errors within the NR uncertainty (represented by the gray region) until around 1 GW cycle before merger. The (uncalibrated) `SEOB-PM` maintains agreement within NR error up to slightly higher velocities for higher mass ratios, and it has much better agreement than when computed on circular orbits [112, 159].

We also extract different spin contributions to the binding energy by combining results from NR simulations for various equal-mass spin combinations [166, 173]: $\mathcal{E}_{\rm SO} = -\frac{1}{6}(-0.6,0)+\frac{8}{3}(0.3,0)-2(0,0)-\frac{1}{2}(0.6,0)+\mathcal{O}(S^3)$ and $\mathcal{E}_{\rm S^2} = \frac{3}{2}(-0.6,0) - 2(0,0) + \frac{3}{2}(0.6,0) - (0.6,-0.6) + \mathcal{O}(S^3)$, where the numbers in brackets correspond to the dimensionless spins (χ_1, χ_2) of the BHs. In Fig. 3 we illustrate the spin-orbit and spin-squared contributions for an equal-mass BBH to the binding energy for the (uncalibrated) `SEOB-PM` at different PM orders, as compared with NR and with the (calibrated) `SEOBNRv5` with (a_6, $d_{\rm SO}$). Despite not being calibrated to NR, `SEOB-PM` shows excellent agreement with the NR results, with a clear convergence towards the NR prediction, as more PM corrections are included. Its accuracy is somewhat better than `SEOBNRv5`, despite the latter model using a Hamiltonian calibrated in the non-spinning (a_6) and spin-orbit coupling ($d_{\rm SO}$) sector (see below).

Calibration to numerical-relativity waveforms – As discussed, the accuracy of EOB inspiral-merger-ringdown waveforms can be enhanced through calibration to NR simulations. For the inspiral-plunge stage, this is generally achieved by introducing in the Hamiltonian high-order (still unknown) PN terms, whose coefficients are tuned to NR, and fitting the time of merger (i.e., the (2,2)-mode's peak time) to NR. In the `SEOBNRv5` model [93], which was built integrating PN results in the Hamiltonian, three calibration parameters were employed: $(\Delta t_{\rm NR}, a_6, d_{\rm SO})$. The parameter $\Delta t_{\rm NR}$ is defined by $t^{22}_{\rm peak} = t_{\rm ISCO} + \Delta t_{\rm NR}$ (see also Eq. (2)), where $t_{\rm ISCO}$ is the time at which $r = r_{\rm ISCO}$, with $r_{\rm ISCO}$ the radius of the Kerr ISCO [174] with the mass and spin of the remnant BH, as given by NR fitting formula [175, 176]. The parameter a_6 is a 5PN correction to the A-potential and $d_{\rm SO}$ is a 4.5PN correction in the gyro-gravitomagnetic coefficients [177]. Here, for the `SEOBNR-PM` model, we do not calibrate high-order PN terms in the non-spinning and spin sectors of the Hamiltonian (3), but we calibrate only the merger's time through $\Delta t_{\rm NR}$. In future work, we will explore NR calibrations tailored to the particular structure of the PM terms. Henceforth, we compare the PM-informed model with several versions of the most recent PN-GSF–informed `SEOBNRv5`, with and without calibration.

Waveform accuracy is often quantified in terms of the mismatch $\mathcal{M}$, defined as 1 minus the overlap between the normalized waveforms, maximized over a relative time and phase shift:

$$\mathcal{M} = 1 - \max_{\phi_0, t_0} \frac{(h_1 \mid h_2)}{\sqrt{(h_1 \mid h_1)\,(h_2 \mid h_2)}}. \tag{6}$$

The overlap is a noise-weighted inner product [178, 179] $(h_1 \mid h_2) \equiv 4\,{\rm Re}\int_{f_l}^{f_h} df \tilde{h}_1(f)\tilde{h}_2^*(f)/S_n(f)$, where $\tilde{h}(f)$ is the Fourier transform of the time-domain signal, the * superscript indicates complex conjugation, and $S_n(f)$ is the power spectral density (PSD) of the detector noise, which we assume to be the design zero-detuned high-power noise PSD of Advanced LIGO [180].

To calibrate the `SEOBNR-PM` model, we closely follow the procedure outlined in Refs. [87, 93, 150]. This pro-

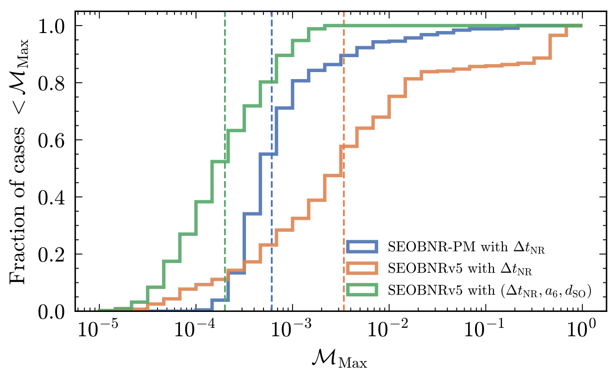

FIG. 4. Cumulative maximum mismatch over the binary's total-mass range $10M_\odot \leq M \leq 300M_\odot$ for the (calibrated) SEOBNR-PM and SEOBNRv5 models. The study uses 441 SXS NR waveforms, and focuses on the $(\ell, m) = (2,2)$ mode. The vertical dashed lines indicate the medians of the mismatch distributions.

cedure essentially consists of determining values of the calibration parameters that minimize a combination of the mismatch and the difference in merger time (defined as the peak of the $(2,2)$-mode amplitude) between EOB and NR waveforms with the same physical parameters (q, χ_1, χ_2). This is carried out in a Bayesian fashion using the Bilby [181] package, and the pySEOBNR code [150]. Finally, we interpolate the best-fit values for each NR simulation across the (q, χ_1, χ_2) parameter space. As said, in our SEOBNR-PM model, we only calibrate the $\Delta t_{\rm NR}$ parameter (see the Supplemental Material for its expression) using 441 NR simulations of aligned-spin BBHs produced with the pseudo-Spectral Einstein code (SpEC) of the Simulating eXtreme Spacetimes (SXS) Collaboration [87, 182–195], which were also employed in Ref. [93] for the SEOBNRv5 model. They cover mass ratios $q = m_1/m_2$ from 1 to 20 in the non-spinning limit, and dimensionless spin values going from $-0.998 \leq \chi_i \leq 0.998$ for $q = 1$ to $-0.5 \leq \chi_1 \leq 0.5,\ \chi_2 = 0$ for $q = 15$.

SEOBNR-PM waveform-model performance – To assess the accuracy of the waveform model, we compute its mismatch against the set of 441 SXS NR simulations, and compare its performance to the SEOBNRv5 $(\Delta t_{\rm NR}, a_6, d_{\rm SO})$ model, as well as, to a version of SEOBNRv5 calibrated only via $\Delta t_{\rm NR}$. Fig. 4 illustrates the cumulative maximum mismatch against the NR simulations over the binary's total-mass range $10M_\odot \leq M \leq 300M_\odot$, for the $(\ell, m) = (2,2)$ mode. The overall mismatch of SEOBNR-PM against NR falls roughly between that of the two SEOBNRv5 variations, with a median value $\mathcal{M}_{\rm median} \sim 6.1 \times 10^{-4}$. This represents a remarkably good agreement. When tuning only $\Delta t_{\rm NR}$, we observe that the accuracy of both SEOBNR-PM and SEOBNRv5 tends to degrade for configurations with large positive spins. This results in a tail of high-mismatch cases above $\sim 1\%$, more pronounced for SEOBNRv5, which includes spin-orbit (3.5PN), spin-square (4PN), and spin-cube (3.5PN) effects at a lower PN order than SEOBNR-PM, which includes spin terms up to 5PM order [196]. Resumming the PM-EOB potentials and introducing calibration parameters could greatly improve SEOBNR-PM's accuracy for these cases, similar to the calibrated SEOBNRv5. We leave this important work to the future.

Conclusions – In this Letter, we took advantage of the flexible and efficient pySEOBNR code [150] and recent prediction for the scattering angle in the EOB formalism [142] to build the first inspiral-merger-ringdown EOB waveform model (SEOBNR-PM) for aligned-spin BHs that uses a PM-informed Hamiltonian (i.e., expanded in G, but at all-orders in the velocity). Importantly, we found that the SEOB-PM non-spinning binding energy, computed along an inspiraling trajectory, at 4PM, and its spin-orbit and spin-spin contributions through 5PM, agree remarkably well with the NR data up to 1 GW cycle before merger (see Figs. 2 and 3). The agreement is comparable and in some cases better than SEOBNRv5, which however was calibrated to NR results [93]. Furthermore, we calibrated SEOBNR-PM to 441 NR simulations provided by the SXS collaboration [87, 182–195] by tuning the (2,2)-mode's peak time (i.e., $\Delta t_{\rm NR}$), and found a median mismatch lower than SEOBNRv5, when the latter is similarly calibrated to NR (see Fig. 4). For now, without optimization, the SEOBNR-PM's evaluation time is an order of magnitude slower than SEOBNRv5.

Considering the recent attention to the two-body gravitational-scattering problem in quantum-field theory, with a slew of new results produced [113–119], we see the development of the SEOBNR-PM model a watershed moment — the first true application of these methods to an astrophysically relevant inspiral-merger-ringdown waveform model. Yet, this is only a first step. Given the relevant progress at 5PM [157], we hope to incorporate the complete 5PM scattering angle into our effective Hamiltonian in the near future. Recent results separating the local from non-local parts of the 4PM angle [197] will likely be crucial for achieving good agreement with NR for highly elliptic bound systems — ultimately, this may be the SEOBNR-PM model's *raison d'être*. In light of the progress in PM fluxes [198–209], PM corrections could also be fed into the EOB radiation-reaction forces and gravitational modes. The SEOB-PM Hamiltonian and fluxes will also need to be extended to the astrophysically relevant precessing-spin case. We leave these tantalizing prospects for future work.

Acknowledgments – We are grateful to Gustav Uhre Jakobsen, Mohammed Khalil, Jan Plefka and Jan Steinhoff for valuable discussions, and to Raffi Enficiaud for his assistance with scientific computing. The work of G.M. and R.P. was supported by the Deutsche Forschungsgemeinschaft (DFG) Projektnummer 417533893/GRK2575 "Rethinking Quantum Field Theory".

SUPPLEMENTAL MATERIAL

Appendix A: PM-informed effective Hamiltonian in the EOB approach

Here we present the effective Hamiltonian $H_{\rm eff}$ (3), which depends on the A-potential and gyro-gravitomagnetic factors:

$$A=\frac{1-2u+\chi_+^2u^2+\Delta A}{1+\chi_+^2u^2(2u+1)}\,,\qquad g_{a_\pm}=\frac{\Delta g_{a_\pm}}{u^2}\,. \tag{A1}$$

These are PM-expanded in Eq. (A2). Corrections to the A-potential incorporate even-in-spin PM corrections:

$$\Delta A^{(n)}=\sum_{s=0}^{\lfloor (n-1)/2\rfloor}\sum_{i=0}^{2s}\alpha^{(n)}_{(2s-i,i)}\delta^{\sigma(i)}\chi_+^{2s-i}\chi_-^{i}\,, \tag{A2}$$

where $\sigma(i)=0,1$ if i is even or odd, respectively. The gyro-gravitomagnetic factors incorporate odd-in-spin PM corrections:

$$\Delta g_{a_+}^{(n)}=\sum_{s=0}^{\lfloor (n-2)/2\rfloor}\sum_{i=0}^{s}\alpha^{(n)}_{(2(s-i)+1,2i)}\chi_+^{2(s-i)}\chi_-^{2i}\,, \tag{A3a}$$

$$\Delta g_{a_-}^{(n)}=\sum_{s=0}^{\lfloor (n-2)/2\rfloor}\sum_{i=0}^{s}\alpha^{(n)}_{(2(s-i),2i+1)}\chi_+^{2(s-i)}\chi_-^{2i}\,. \tag{A3b}$$

The dimensionless parameters $\alpha^{(n)}_{(i,j)}$ are functions of $\gamma=E_{\rm eff}/\mu$ and the symmetric mass ratio ν.

We now provide the deformation coefficients required in order to fully specify the effective Hamiltonian for non-spinning configurations. For the full spinning, we refer the interested reader to the ancillary file attached to the `arXiv` submission of this Letter that contains the complete EOB and effective Hamiltonians. Firstly, the 2PM non-spinning deformation is

$$\alpha^{(2)}_{(0,0)}=\frac{3(\Gamma-1)(5\gamma^2-1)}{2\gamma^2\Gamma}\,, \tag{A4}$$

where $\Gamma=\sqrt{1+2\nu(\gamma-1)}$ is the dimensionless total energy. Next, at 3PM order we require

$$\alpha^{(3)}_{(0,0)}=\frac{9(\Gamma-1)\left(30\gamma^4-31\gamma^2+5\right)+2\nu\left(-214\gamma^5+270\gamma^4+323\gamma^3-279\gamma^2-145\gamma+45\right)}{6\gamma^2\left(\gamma^2-1\right)\Gamma^2}+\frac{4\nu\left(4\gamma^4-12\gamma^2-3\right)}{\gamma^2\Gamma^2}\frac{\arccos\gamma}{\sqrt{1-\gamma^2}}\,. \tag{A5}$$

Here, we have replaced $\mathrm{arccosh}(\gamma)/\sqrt{\gamma^2-1}$ by $\arccos(\gamma)/\sqrt{1-\gamma^2}$. Finally, at 4PM order we encounter

$$\begin{aligned}
\alpha^{(4)}_{(0,0)}=&\frac{7\nu\left(380\gamma^2+169\right)}{8(\gamma-1)\gamma^2\Gamma^3}\mathrm{E}^2\left(\frac{\gamma-1}{\gamma+1}\right)+\frac{\left(1200\gamma^2+2095\gamma+834\right)\nu}{4\gamma^2\left(\gamma^2-1\right)\Gamma^3}\mathrm{K}^2\left(\frac{\gamma-1}{\gamma+1}\right)\\
&+\frac{\left(-1200\gamma^3-2660\gamma^2-2929\gamma-1183\right)\nu}{4\gamma^2\left(\gamma^2-1\right)\Gamma^3}\mathrm{E}\left(\frac{\gamma-1}{\gamma+1}\right)\mathrm{K}\left(\frac{\gamma-1}{\gamma+1}\right)\\
&+\frac{\left(-25\gamma^6+30\gamma^4+111\gamma^2+20\right)\nu}{\gamma^2\Gamma^3}\mathrm{Li}_2\left(\frac{1-\gamma}{1+\gamma}\right)+\frac{(\gamma+1)\left(25\gamma^5-25\gamma^4-5\gamma^3+65\gamma^2+64\gamma+12\right)\nu}{2\gamma^2\Gamma^3}\mathrm{Li}_2\left(\frac{\gamma-1}{\gamma+1}\right)\\
&+\frac{\left(35\gamma^4+120\gamma^3+90\gamma^2+152\gamma+27\right)\nu}{2\gamma^2\Gamma^3}\log^2\left(\frac{\gamma+1}{2}\right)-\frac{4\left(2\gamma^2-3\right)\left(15\gamma^2-15\gamma+4\right)\nu}{\gamma(\gamma+1)\Gamma^3}\frac{\mathrm{Ti}_2\left(\sqrt{\frac{1-\gamma}{1+\gamma}}\right)}{\sqrt{1-\gamma^2}}\\
&+\frac{\left(2\gamma^2-3\right)^2\left(35\gamma^4-30\gamma^2+11\right)\nu}{8\left(\gamma^2-1\right)^3\Gamma^3}\arccos^2\gamma+\frac{2\left(75\gamma^6-140\gamma^4-283\gamma^2-852\right)\nu}{3\gamma\left(\gamma^2-1\right)\Gamma^3}\log(\gamma)\\
&+\frac{\left(210\gamma^6-552\gamma^5+339\gamma^4-912\gamma^3+3148\gamma^2-3336\gamma+1151\right)\nu}{12\gamma^2\left(\gamma^2-1\right)\Gamma^3}\log\left(\frac{u}{4}\right)\\
&+\left(\frac{\left(-35\gamma^4-60\gamma^3+150\gamma^2-76\gamma+5\right)\nu}{2\gamma^2\Gamma^3}\log\left(\frac{u}{4}\right)\right.\\
&\quad\left.+\frac{\left(-75\gamma^7+416\gamma^5+612\gamma^4+739\gamma^3+136\gamma^2+2520\gamma+152\right)\nu}{3\gamma^2\left(\gamma^2-1\right)\Gamma^3}\right)\log\left(\frac{\gamma+1}{2}\right)
\end{aligned} \tag{A6}$$

$$
\begin{aligned}
&+\Bigg(\frac{\left(-420\gamma^9+96\gamma^8-48\gamma^7+5328\gamma^6-5279\gamma^5-1584\gamma^4+7142\gamma^3-9360\gamma^2+3453\gamma+720\right)\nu}{12\gamma^2(\gamma^2-1)^2\Gamma^3}\\
&\quad-\frac{48\left(7\gamma^2-5\right)\left(4\gamma^4-12\gamma^2-3\right)(\Gamma-1)\nu}{12\gamma^2(\gamma^2-1)\Gamma^3}\\
&\quad-\frac{\left(2\gamma^2-3\right)\left(35\gamma^4-30\gamma^2+11\right)\nu}{4\gamma(1-\gamma^2)\Gamma^3}\log\left(\frac{u}{4}\right)+\frac{4\left(2\gamma^2-3\right)\left(15\gamma^2+2\right)\nu}{\gamma(1-\gamma^2)\Gamma^3}\log\left(\frac{\gamma+1}{2}\right)\Bigg)\frac{\arccos\gamma}{\sqrt{1-\gamma^2}}\\
&+(\Gamma-1)\Bigg(\frac{5115\gamma^8-9537\gamma^6+5657\gamma^4-1115\gamma^2+72}{16\gamma^4\left(\gamma^2-1\right)^2\Gamma^3}\\
&\quad+\frac{\left(8159\gamma^8-3136\gamma^7-23601\gamma^6-3360\gamma^5+15409\gamma^4+4000\gamma^3-1995\gamma^2+108\right)\nu}{24(\gamma-1)\gamma^4(\gamma+1)^2\Gamma^3}\Bigg)\\
&+\frac{\nu}{144\gamma^9\left(\gamma^2-1\right)^2\Gamma^3}\Big(-600\pi^2\gamma^{17}+3600\gamma^{16}+480\left(9+4\pi^2\right)\gamma^{15}+2\left(720\pi^2-28843\right)\gamma^{14}+\left(36759-5136\pi^2\right)\gamma^{13}\\
&\quad+\left(44698-1056\pi^2\right)\gamma^{12}+\left(6624\pi^2-43235\right)\gamma^{11}+\left(7702-2208\pi^2\right)\gamma^{10}-5\left(2155+504\pi^2\right)\gamma^9\\
&\quad+2\left(23947+912\pi^2\right)\gamma^8-\left(45605+288\pi^2\right)\gamma^7+12701\gamma^6+648\gamma^5-1471\gamma^4+207\gamma^2-45\Big)\,,
\end{aligned}
$$

where $\mathrm{Ti}_2(x) := \int_0^x (\mathrm{d}t/t)\arctan t$ is the inverse tangent integral. This expression also includes $\log(u)$, which is obtained by taking the bound circular-orbit limit (at leading-PN order) of $\log(1-\gamma^2)$ (i.e., the real part of $\log(\gamma^2-1)$). This ensures that the coefficient is real for $\gamma<1$. Finally, to complete the non-spinning dynamics we require the 4PN correction coefficient $\Delta A^{\rm 4PN}$ (5). This includes three numerical coefficients:

$$
c_1=\frac{\nu}{15}(-1411+296\gamma_{\rm E}-1328\log 2+2187\log 3)\,, \tag{A7a}
$$

$$
c_2=\frac{9\nu^3}{4}+\frac{\nu^2}{192}\left(615\pi^2-16408\right) +\nu\left(-\frac{51187}{360}+\frac{136\gamma_{\rm E}}{3}+\frac{1571\pi^2}{6144}-\frac{856\log 2}{15}+\frac{729\log 3}{5}\right), \tag{A7b}
$$

$$
c_3=-\frac{68\nu}{3}\,, \tag{A7c}
$$

with $\gamma_{\rm E}\approx 0.557$ Euler's constant.

Appendix B: Interpreting γ within $\alpha^{(n)}_{(i,j)}$

The effective Hamiltonian $H_{\rm eff}$ (3) contains deformation parameters $\alpha^{(n)}_{(i,j)}$ that depend on $\gamma=E_{\rm eff}/\mu$ (i.e., the Hamiltonian technically depends on itself). In principle, one should therefore solve for $E_{\rm eff}=H_{\rm eff}$ as a function of the kinematic variables (r,p_r,p_ϕ); however, given the highly non-trivial dependence on γ on the right-hand side of Eq. (3), not to mention the appearance of special functions including dilogarithms and elliptics, such an approach is not practical. While one might also try solving for the Hamiltonian numerically at a given phase-space point, this approach will not lead to an efficient implementation within `pySEOBNR`.

Instead, building on the approach taken in Ref. [112, 159] for the non-spinning case, we interpret γ as the effective energy expanded only up to whatever PM and/or spin order is necessary to ensure that the complete resummed Hamiltonian $H_{\rm EOB}=M\sqrt{1+2\nu(H_{\rm eff}/\mu-1)}$ is consistent with the known PM and spin results. The effective Hamiltonian may be perturbatively expanded as

$$
\gamma=\gamma_{\rm Kerr}+\sum_{n\geq 2}\sum_{s\geq 0}\Delta^{(n)}_{(s)}(\gamma_{\rm Kerr}) \tag{B1}
$$

with deformations $\Delta^{(n)}_{(s)}(\gamma_{\rm Kerr})$, characterized by PM order n and spin order s, depending on $\gamma_{\rm Kerr}=H_{\rm Kerr}/\mu$. The Kerr Hamiltonian here is

$$
H_{\rm Kerr}=\frac{2Mp_\phi a}{r^3+a^2(r+2M)} +\sqrt{A^{\rm Kerr}\left(\mu^2+\frac{p_\phi^2}{r^2}+(1+B^{\rm Kerr}_{\rm np})p_r^2+B^{\rm Kerr}_{\rm npa}\frac{p_\phi^2a^2}{r^2}\right)}\,, \tag{B2}
$$

where we identify the total spin $a=a_+$ in the EOB. The three functions appearing in the Kerr Hamiltonian are

$$
A^{\rm Kerr}=\frac{1-2u+\chi^2u^2}{1+\chi^2u^2(2u+1)}\,, \tag{B3a}
$$

$$
B^{\rm Kerr}_{\rm np}=\chi^2u^2-2u\,, \tag{B3b}
$$

$$
B^{\rm Kerr}_{\rm npa}=-\frac{1+2u}{r^2+a^2(1+2u)}\,. \tag{B3c}
$$

For our purposes, expressions for the following five deformations (up to 3PM order) are sufficient:

$$\Delta^{(2)}_{(0)} = \frac{u^2}{2}\alpha^{(2)}_{(0,0)}(\gamma_{\rm Kerr})\gamma_{\rm Kerr}\,, \tag{B4a}$$

$$\Delta^{(2)}_{(1)} = \ell u^3\left((\alpha^{(2)}_{(1,0)}(\gamma_{\rm Kerr})-2)a_+ + \alpha^{(2)}_{(0,1)}(\gamma_{\rm Kerr})\delta a_-\right), \tag{B4b}$$

$$\Delta^{(3)}_{(0)} = \frac{u^3}{2}\left(2\alpha^{(2)}_{(0,0)}(\gamma_{\rm Kerr})+\alpha^{(3)}_{(0,0)}(\gamma_{\rm Kerr})\right)\gamma_{\rm Kerr}\,, \tag{B4c}$$

$$\Delta^{(3)}_{(1)} = \ell u^4\left(\alpha^{(3)}_{(1,0)}(\gamma_{\rm Kerr})a_+ + \alpha^{(3)}_{(0,1)}(\gamma_{\rm Kerr})\delta a_-\right), \tag{B4d}$$

$$\Delta^{(3)}_{(2)} = \frac{u^3}{2}\left(\alpha^{(3)}_{(2,0)}(\gamma_{\rm Kerr})a_+^2 + \alpha^{(3)}_{(0,2)}(\gamma_{\rm Kerr})a_-^2 + \alpha^{(3)}_{(1,1)}(\gamma_{\rm Kerr})\delta a_+ a_-\right)\gamma_{\rm Kerr}\,, \tag{B4e}$$

Within a given coefficient $\alpha^{(n)}_{(i,j)}$ we use whatever deformations in Eq. (B4) are required. The explicit coefficient-by-coefficient replacements used in our model are

$$\begin{aligned}
\alpha^{(2)}_{(0,0)}(\gamma):&\quad \gamma\to\gamma_{\rm Kerr}+\Delta^{(2)}_{(0)}+\Delta^{(2)}_{(1)}+\Delta^{(3)}_{(1)}+\Delta^{(3)}_{(2)}\,,\\
\alpha^{(3)}_{(0,0)}(\gamma):&\quad \gamma\to\gamma_{\rm Kerr}+\Delta^{(2)}_{(1)}\,,\\
\alpha^{(2)}_{(1,0)}(\gamma):&\quad \gamma\to\gamma_{\rm Kerr}+\Delta^{(2)}_{(0)}+\Delta^{(2)}_{(1)}+\Delta^{(3)}_{(0)}+\Delta^{(3)}_{(1)}+\Delta^{(3)}_{(2)}\,,\\
\alpha^{(2)}_{(0,1)}(\gamma):&\quad \gamma\to\gamma_{\rm Kerr}+\Delta^{(2)}_{(0)}+\Delta^{(2)}_{(1)}+\Delta^{(3)}_{(0)}+\Delta^{(3)}_{(1)}+\Delta^{(3)}_{(2)}\,,\\
\alpha^{(3)}_{(1,0)}(\gamma):&\quad \gamma\to\gamma_{\rm Kerr}+\Delta^{(2)}_{(0)}+\Delta^{(2)}_{(1)}\,,\\
\alpha^{(3)}_{(0,1)}(\gamma):&\quad \gamma\to\gamma_{\rm Kerr}+\Delta^{(2)}_{(0)}+\Delta^{(2)}_{(1)}\,,\\
\alpha^{(3)}_{(2,0)}(\gamma):&\quad \gamma\to\gamma_{\rm Kerr}+\Delta^{(2)}_{(0)}+\Delta^{(2)}_{(1)}\,,\\
\alpha^{(3)}_{(0,2)}(\gamma):&\quad \gamma\to\gamma_{\rm Kerr}+\Delta^{(2)}_{(0)}+\Delta^{(2)}_{(1)}\,,\\
\alpha^{(3)}_{(1,1)}(\gamma):&\quad \gamma\to\gamma_{\rm Kerr}+\Delta^{(2)}_{(0)}+\Delta^{(2)}_{(1)}\,,
\end{aligned} \tag{B5}$$

and in all other cases we replace $\gamma\to\gamma_{\rm Kerr}$ (including $\Delta A^{\rm 4PN}$). For example, as $\alpha^{(3)}_{(1,0)}$ appears at 3PM order in $H_{\rm eff}$, we need all corrections up to 2PM order in order to ensure that our Hamiltonian remains correct up to 5PM. An exception is the two non-spinning parameters $\alpha^{(2)}_{(0,0)}$ and $\alpha^{(3)}_{(0,0)}$, wherein we do not include $\Delta^{(3)}_{(0)}$ and $\Delta^{(2)}_{(0)}$, respectively, as the non-spinning 5PM contribution is not included from known perturbative PM results. We instead correct using the 4PN term $\Delta A^{\rm 4PN}$. The result of this procedure is an effective Hamiltonian that now depends *explicitly* on (r,p_r,p_ϕ). As this procedure changes the nature of the resummation, our Hamiltonian is therefore different from the one encountered in the `SEOB-PM` scattering model [142].

A consequence of treating γ via Eq. (B1) is that it vanishes wherever $H_{\rm Kerr}$ does. For example, in the non-spinning limit, this leads to a pole at the Schwarzschild horizon $r=2M$ in the $\alpha^{(n)}_{(i,j)}$ coefficients (A2), which contain powers of $1/\gamma$, and consequently in the A-potential. This would not necessarily occur if γ was defined as $\gamma=E_{\rm eff}/\mu$, as the effective Hamiltonian does not need to vanish at the horizon. Since the pole appears at a very small separation, it does not prevent evolving the binary until the merger time (which occurs before the time of horizon crossing) and obtaining an accurate inspiral-merger-ringdown waveform. However, the presence of the pole impacts the shape of the A-potential (and of the overall Hamiltonian) in the strong-field regime and might limit the flexibility that can be gained from incorporating higher-order calibration parameters in the EOB Hamiltonian. For example, adding a 5PN calibration parameter a_6u^6 to the A-potential via Eq. (5), similar to the one used in `SEOBNRv5`, does not improve the agreement of the non-spinning `SEOBNR-PM` against NR simulations as effectively as the corresponding parameter in `SEOBNRv5`. In the future, we will explore different strategies to interpret γ, and seek for a more suitable choice of the NR calibration parameters tailored to the particular structure of the PM terms, which can enable a more effective NR calibration of the spinning model.

Appendix C: Fits of the NR-calibration parameters

Since NR simulations are only available at discrete parameter values, to generate the model for generic configurations we need to fit the NR calibration parameter $\Delta t_{\rm NR}$ across the (q,χ_1,χ_2), or equivalently (ν,χ_+,χ_-), parameter space. We do this hierarchically, fitting first non-spinning and then aligned-spin configurations, using the same ansatz as in `SEOBNRv5`. The final expression for `SEOBNR-PM` reads

$$\begin{aligned}
\Delta t_{\rm NR} =\ & \nu^{-1/5+12.73\nu}\big(113115.96\nu^3-25626.22\nu^2\\
&-1457.38\nu-60.17\big)\\
&+\nu^{-1/5}\big(195.45\nu^2\chi_+-190.15\nu^2\chi_-+52.14\nu\chi_+^2\\
&-72.80\nu\chi_+\chi_--72.56\nu\chi_++50.90\nu\chi_-^2\\
&-15.76\nu\chi_-+0.24\chi_+^4-1.51\chi_+^3+4.23\chi_+^2\chi_-\\
&-10.51\chi_+^2+1.22\chi_+\chi_-^2+18.89\chi_+\chi_-\\
&+10.10\chi_+-10.50\chi_-^2+17.08\chi_-\big)\,.
\end{aligned} \tag{C1}$$

For completeness, we also report the fit used in the variation of the `SEOBNRv5` model shown in Fig. 4, in which only this parameter is tuned to NR:

$$\begin{aligned}
\Delta t_{\rm NR} =\ & \nu^{-1/5+4.97\nu}\big(-4091.55\nu^3+2493.06\nu^2\\
&-205.61\nu-53.99\big)\\
&+\nu^{-1/5}\big(45.32\nu^2\chi_+-874.81\nu^2\chi_-+71.25\nu\chi_+^2\\
&+65.96\nu\chi_+\chi_-+3.72\nu\chi_+-100.55\nu\chi_-^2\\
&+160.60\nu\chi_--89.85\chi_+^4-43.49\chi_+^3-1.07\chi_+^2\chi_-\\
&+59.49\chi_+^2+0.94\chi_+\chi_-^2-17.51\chi_+\chi_-\\
&+36.27\chi_++26.08\chi_-^2+15.37\chi_-\big)\,.
\end{aligned} \tag{C2}$$

The complete `SEOBNRv5` model also contains calibrations of the a_6 and $d_{\rm SO}$ parameters, together with a different fit for $\Delta t_{\rm NR}$ [93].

[1] B. P. Abbott *et al.* (LIGO Scientific, Virgo), "Observation of Gravitational Waves from a Binary Black Hole Merger," Phys. Rev. Lett. **116**, 061102 (2016), arXiv:1602.03837 [gr-qc].

[2] J. Aasi *et al.* (LIGO Scientific), "Advanced LIGO," Class. Quant. Grav. **32**, 074001 (2015), arXiv:1411.4547 [gr-qc].

[3] F. Acernese *et al.* (VIRGO), "Advanced Virgo: a second-generation interferometric gravitational wave detector," Class. Quant. Grav. **32**, 024001 (2015), arXiv:1408.3978 [gr-qc].

[4] T. Akutsu *et al.* (KAGRA), "Overview of KAGRA: Detector design and construction history," PTEP **2021**, 05A101 (2021), arXiv:2005.05574 [physics.ins-det].

[5] B. P. Abbott *et al.* (LIGO Scientific, Virgo), "GW170817: Observation of Gravitational Waves from a Binary Neutron Star Inspiral," Phys. Rev. Lett. **119**, 161101 (2017), arXiv:1710.05832 [gr-qc].

[6] R. Abbott *et al.* (KAGRA, VIRGO, LIGO Scientific), "GWTC-3: Compact Binary Coalescences Observed by LIGO and Virgo during the Second Part of the Third Observing Run," Phys. Rev. X **13**, 041039 (2023), arXiv:2111.03606 [gr-qc].

[7] Alexander H. Nitz, Sumit Kumar, Yi-Fan Wang, Shilpa Kastha, Shichao Wu, Marlin Schäfer, Rahul Dhurkunde, and Collin D. Capano, "4-OGC: Catalog of Gravitational Waves from Compact Binary Mergers," Astrophys. J. **946**, 59 (2023), arXiv:2112.06878 [astro-ph.HE].

[8] Seth Olsen, Tejaswi Venumadhav, Jonathan Mushkin, Javier Roulet, Barak Zackay, and Matias Zaldarriaga, "New binary black hole mergers in the LIGO-Virgo O3a data," Phys. Rev. D **106**, 043009 (2022), arXiv:2201.02252 [astro-ph.HE].

[9] Ajit Kumar Mehta, Seth Olsen, Digvijay Wadekar, Javier Roulet, Tejaswi Venumadhav, Jonathan Mushkin, Barak Zackay, and Matias Zaldarriaga, "New binary black hole mergers in the LIGO-Virgo O3b data," (2023), arXiv:2311.06061 [gr-qc].

[10] Digvijay Wadekar, Javier Roulet, Tejaswi Venumadhav, Ajit Kumar Mehta, Barak Zackay, Jonathan Mushkin, Seth Olsen, and Matias Zaldarriaga, "New black hole mergers in the LIGO-Virgo O3 data from a gravitational wave search including higher-order harmonics," (2023), arXiv:2312.06631 [gr-qc].

[11] R. Abbott *et al.* (KAGRA, VIRGO, LIGO Scientific), "Population of Merging Compact Binaries Inferred Using Gravitational Waves through GWTC-3," Phys. Rev. X **13**, 011048 (2023), arXiv:2111.03634 [astro-ph.HE].

[12] B. P. Abbott *et al.* (LIGO Scientific, Virgo), "GW170817: Measurements of neutron star radii and equation of state," Phys. Rev. Lett. **121**, 161101 (2018), arXiv:1805.11581 [gr-qc].

[13] B. P. Abbott *et al.* (LIGO Scientific, Virgo, 1M2H, Dark Energy Camera GW-E, DES, DLT40, Las Cumbres Observatory, VINROUGE, MASTER), "A gravitational-wave standard siren measurement of the Hubble constant," Nature **551**, 85–88 (2017), arXiv:1710.05835 [astro-ph.CO].

[14] R. Abbott *et al.* (LIGO Scientific, Virgo, KAGRA), "Constraints on the Cosmic Expansion History from GWTC–3," Astrophys. J. **949**, 76 (2023), arXiv:2111.03604 [astro-ph.CO].

[15] B. P. Abbott *et al.* (LIGO Scientific, Virgo), "Tests of general relativity with GW150914," Phys. Rev. Lett. **116**, 221101 (2016), [Erratum: Phys.Rev.Lett. 121, 129902 (2018)], arXiv:1602.03841 [gr-qc].

[16] R. Abbott *et al.* (LIGO Scientific, Virgo), "Tests of general relativity with binary black holes from the second LIGO-Virgo gravitational-wave transient catalog," Phys. Rev. D **103**, 122002 (2021), arXiv:2010.14529 [gr-qc].

[17] R. Abbott *et al.* (LIGO Scientific, VIRGO, KAGRA), "Tests of General Relativity with GWTC-3," (2021), arXiv:2112.06861 [gr-qc].

[18] M. Punturo *et al.*, "The Einstein Telescope: A third-generation gravitational wave observatory," Class. Quant. Grav. **27**, 194002 (2010).

[19] Vicky Kalogera *et al.*, "The Next Generation Global Gravitational Wave Observatory: The Science Book," (2021), arXiv:2111.06990 [gr-qc].

[20] David Reitze *et al.*, "Cosmic Explorer: The U.S. Contribution to Gravitational-Wave Astronomy beyond LIGO," Bull. Am. Astron. Soc. **51**, 035 (2019), arXiv:1907.04833 [astro-ph.IM].

[21] Pau Amaro-Seoane *et al.* (LISA), "Laser Interferometer Space Antenna," (2017), arXiv:1702.00786 [astro-ph.IM].

[22] Jun Luo *et al.* (TianQin), "TianQin: a space-borne gravitational wave detector," Class. Quant. Grav. **33**, 035010 (2016), arXiv:1512.02076 [astro-ph.IM].

[23] Yue-Liang Wu *et al.* (Taiji Scientific), "China's first step towards probing the expanding universe and the nature of gravity using a space borne gravitational wave antenna," Commun. Phys. **4**, 34 (2021).

[24] Ssohrab Borhanian and B. S. Sathyaprakash, "Listening to the Universe with Next Generation Ground-Based Gravitational-Wave Detectors," (2022), arXiv:2202.11048 [gr-qc].

[25] Arnab Dhani, Sebastian Völkel, Alessandra Buonanno, Hector Estelles, Jonathan Gair, Harald P. Pfeiffer, Lorenzo Pompili, and Alexandre Toubiana, "Systematic Biases in Estimating the Properties of Black Holes Due to Inaccurate Gravitational-Wave Models," (2024), arXiv:2404.05811 [gr-qc].

[26] B. P. Abbott *et al.* (KAGRA, LIGO Scientific, Virgo, VIRGO), "Prospects for observing and localizing gravitational-wave transients with Advanced LIGO, Advanced Virgo and KAGRA," Living Rev. Rel. **21**, 3 (2018), arXiv:1304.0670 [gr-qc].

[27] Matthew Evans *et al.*, "A Horizon Study for Cosmic Explorer: Science, Observatories, and Community," (2021), arXiv:2109.09882 [astro-ph.IM].

[28] Slavko Bogdanov *et al.*, "Snowmass 2021 Cosmic Frontier White Paper: The Dense Matter Equation of State and QCD Phase Transitions," in *Snowmass 2021* (2022) arXiv:2209.07412 [astro-ph.HE].

[29] Monica Colpi *et al.*, "LISA Definition Study Report," (2024), arXiv:2402.07571 [astro-ph.CO].

[30] Alexandre Toubiana, Lorenzo Pompili, Alessandra Buonanno, Jonathan R. Gair, and Michael L. Katz, "Measuring source properties and quasinormal mode frequen-

cies of heavy massive black-hole binaries with LISA," Phys. Rev. D **109**, 104019 (2024), arXiv:2307.15086 [gr-qc].

[31] Anuradha Gupta *et al.*, "Possible Causes of False General Relativity Violations in Gravitational Wave Observations," (2024), arXiv:2405.02197 [gr-qc].

[32] Frans Pretorius, "Evolution of binary black hole spacetimes," Phys. Rev. Lett. **95**, 121101 (2005), arXiv:gr-qc/0507014.

[33] Manuela Campanelli, C. O. Lousto, P. Marronetti, and Y. Zlochower, "Accurate evolutions of orbiting black-hole binaries without excision," Phys. Rev. Lett. **96**, 111101 (2006), arXiv:gr-qc/0511048.

[34] John G. Baker, Joan Centrella, Dae-Il Choi, Michael Koppitz, and James van Meter, "Gravitational wave extraction from an inspiraling configuration of merging black holes," Phys. Rev. Lett. **96**, 111102 (2006), arXiv:gr-qc/0511103.

[35] Toshifumi Futamase and Yousuke Itoh, "The post-Newtonian approximation for relativistic compact binaries," Living Rev. Rel. **10**, 2 (2007).

[36] Luc Blanchet, "Gravitational Radiation from Post-Newtonian Sources and Inspiralling Compact Binaries," Living Rev. Rel. **17**, 2 (2014), arXiv:1310.1528 [gr-qc].

[37] Rafael A. Porto, "The effective field theorist's approach to gravitational dynamics," Phys. Rept. **633**, 1–104 (2016), arXiv:1601.04914 [hep-th].

[38] Schäfer, Gerhard and Jaranowski, Piotr, "Hamiltonian formulation of general relativity and post-Newtonian dynamics of compact binaries," Living Rev. Rel. **21**, 7 (2018), arXiv:1805.07240 [gr-qc].

[39] Michèle Levi, "Effective Field Theories of Post-Newtonian Gravity: A comprehensive review," Rept. Prog. Phys. **83**, 075901 (2020), arXiv:1807.01699 [hep-th].

[40] Piotr Jaranowski and Gerhard Schaefer, "Third post-Newtonian higher order ADM Hamilton dynamics for two-body point mass systems," Phys. Rev. D **57**, 7274–7291 (1998), [Erratum: Phys.Rev.D 63, 029902 (2001)], arXiv:gr-qc/9712075.

[41] Damour, Thibault and Jaranowski, Piotr and Schäfer, Gerhard, "Nonlocal-in-time action for the fourth post-Newtonian conservative dynamics of two-body systems," Phys. Rev. **D89**, 064058 (2014), arXiv:1401.4548 [gr-qc].

[42] Piotr Jaranowski and Gerhard Schäfer, "Derivation of local-in-time fourth post-Newtonian ADM Hamiltonian for spinless compact binaries," Phys. Rev. D **92**, 124043 (2015), arXiv:1508.01016 [gr-qc].

[43] Laura Bernard, Luc Blanchet, Alejandro Bohé, Guillaume Faye, and Sylvain Marsat, "Fokker action of nonspinning compact binaries at the fourth post-Newtonian approximation," Phys. Rev. D **93**, 084037 (2016), arXiv:1512.02876 [gr-qc].

[44] Laura Bernard, Luc Blanchet, Alejandro Bohé, Guillaume Faye, and Sylvain Marsat, "Energy and periastron advance of compact binaries on circular orbits at the fourth post-Newtonian order," Phys. Rev. **D95**, 044026 (2017), arXiv:1610.07934 [gr-qc].

[45] Damour, Thibault and Jaranowski, Piotr and Schäfer, Gerhard, "Conservative dynamics of two-body systems at the fourth post-Newtonian approximation of general relativity," Phys. Rev. **D93**, 084014 (2016), arXiv:1601.01283 [gr-qc].

[46] Luc Blanchet, Guillaume Faye, Quentin Henry, François Larrouturou, and David Trestini, "Gravitational-wave flux and quadrupole modes from quasicircular nonspinning compact binaries to the fourth post-Newtonian order," Phys. Rev. D **108**, 064041 (2023), arXiv:2304.11186 [gr-qc].

[47] Luc Blanchet, Guillaume Faye, Quentin Henry, François Larrouturou, and David Trestini, "Gravitational-Wave Phasing of Quasicircular Compact Binary Systems to the Fourth-and-a-Half Post-Newtonian Order," Phys. Rev. Lett. **131**, 121402 (2023), arXiv:2304.11185 [gr-qc].

[48] Stefano Foffa and Riccardo Sturani, "Conservative dynamics of binary systems to fourth Post-Newtonian order in the EFT approach I: Regularized Lagrangian," Phys. Rev. **D100**, 024047 (2019), arXiv:1903.05113 [gr-qc].

[49] Stefano Foffa, Rafael A. Porto, Ira Rothstein, and Riccardo Sturani, "Conservative dynamics of binary systems to fourth Post-Newtonian order in the EFT approach II: Renormalized Lagrangian," Phys. Rev. **D100**, 024048 (2019), arXiv:1903.05118 [gr-qc].

[50] Blümlein, J. and Maier, A. and Marquard, P. and Schäfer, G., "Fourth post-Newtonian Hamiltonian dynamics of two-body systems from an effective field theory approach," Nucl. Phys. B **955**, 115041 (2020), arXiv:2003.01692 [gr-qc].

[51] K. Westpfahl and M. Goller, "Gravitational scattering of two relativistic particles in postlinear approximation," Lett. Nuovo Cim. **26**, 573–576 (1979).

[52] K. Westpfahl and H. Hoyler, "Gravitational bremsstrahlung in post-linear fast-motion approximation," Lett. Nuovo Cim. **27**, 581–585 (1980).

[53] LLuis Bel, T. Damour, N. Deruelle, J. Ibanez, and J. Martin, "Poincaré-invariant gravitational field and equations of motion of two pointlike objects: The post-linear approximation of general relativity," Gen. Rel. Grav. **13**, 963–1004 (1981).

[54] Konradin Westpfahl, "High-Speed Scattering of Charged and Uncharged Particles in General Relativity," Fortsch. Phys. **33**, 417–493 (1985).

[55] Gerhard Schäfer, "The adm hamiltonian at the postlinear approximation," General relativity and gravitation **18**, 255–270 (1986).

[56] Tomas Ledvinka, Gerhard Schaefer, and Jiri Bicak, "Relativistic Closed-Form Hamiltonian for Many-Body Gravitating Systems in the Post-Minkowskian Approximation," Phys. Rev. Lett. **100**, 251101 (2008), arXiv:0807.0214 [gr-qc].

[57] Alessandra Buonanno, Mohammed Khalil, Donal O'Connell, Radu Roiban, Mikhail P. Solon, and Mao Zeng, "Snowmass White Paper: Gravitational Waves and Scattering Amplitudes," in *2022 Snowmass Summer Study* (2022) arXiv:2204.05194 [hep-th].

[58] Gabriele Travaglini *et al.*, "The SAGEX review on scattering amplitudes*," J. Phys. A **55**, 443001 (2022), arXiv:2203.13011 [hep-th].

[59] N. E. J. Bjerrum-Bohr, P. H. Damgaard, L. Plante, and P. Vanhove, "Chapter 13: Post-Minkowskian expansion from scattering amplitudes," J. Phys. A **55**, 443014 (2022), arXiv:2203.13024 [hep-th].

[60] David A. Kosower, Ricardo Monteiro, and Donal O'Connell, "Chapter 14: Classical gravity from scattering amplitudes," J. Phys. A **55**, 443015 (2022),

arXiv:2203.13025 [hep-th].
[61] Yasushi Mino, Misao Sasaki, and Takahiro Tanaka, "Gravitational radiation reaction to a particle motion," Phys. Rev. D **55**, 3457–3476 (1997), arXiv:gr-qc/9606018.
[62] Theodore C. Quinn and Robert M. Wald, "An Axiomatic approach to electromagnetic and gravitational radiation reaction of particles in curved space-time," Phys. Rev. D **56**, 3381–3394 (1997), arXiv:gr-qc/9610053.
[63] Leor Barack, Yasushi Mino, Hiroyuki Nakano, Amos Ori, and Misao Sasaki, "Calculating the gravitational selfforce in Schwarzschild space-time," Phys. Rev. Lett. **88**, 091101 (2002), arXiv:gr-qc/0111001.
[64] Leor Barack and Amos Ori, "Gravitational selfforce on a particle orbiting a Kerr black hole," Phys. Rev. Lett. **90**, 111101 (2003), arXiv:gr-qc/0212103.
[65] Samuel E. Gralla and Robert M. Wald, "A Rigorous Derivation of Gravitational Self-force," Class. Quant. Grav. **25**, 205009 (2008), [Erratum: Class.Quant.Grav. 28, 159501 (2011)], arXiv:0806.3293 [gr-qc].
[66] Steven L. Detweiler, "A Consequence of the gravitational self-force for circular orbits of the Schwarzschild geometry," Phys. Rev. **D77**, 124026 (2008), arXiv:0804.3529 [gr-qc].
[67] Tobias S. Keidl, Abhay G. Shah, John L. Friedman, Dong-Hoon Kim, and Larry R. Price, "Gravitational Self-force in a Radiation Gauge," Phys. Rev. D **82**, 124012 (2010), [Erratum: Phys.Rev.D 90, 109902 (2014)], arXiv:1004.2276 [gr-qc].
[68] Maarten van de Meent, "Gravitational self-force on generic bound geodesics in Kerr spacetime," Phys. Rev. D **97**, 104033 (2018), arXiv:1711.09607 [gr-qc].
[69] Adam Pound, "Second-order gravitational self-force," Phys. Rev. Lett. **109**, 051101 (2012), arXiv:1201.5089 [gr-qc].
[70] Adam Pound, Barry Wardell, Niels Warburton, and Jeremy Miller, "Second-order self-force calculation of the gravitational binding energy in compact binaries," Phys. Rev. Lett. **124**, 021101 (2020), arXiv:1908.07419 [gr-qc].
[71] Samuel E. Gralla and Kunal Lobo, "Self-force effects in post-Minkowskian scattering," Class. Quant. Grav. **39**, 095001 (2022), arXiv:2110.08681 [gr-qc].
[72] Adam Pound and Barry Wardell, "Black hole perturbation theory and gravitational self-force," (2021), arXiv:2101.04592 [gr-qc].
[73] Niels Warburton, Adam Pound, Barry Wardell, Jeremy Miller, and Leanne Durkan, "Gravitational-Wave Energy Flux for Compact Binaries through Second Order in the Mass Ratio," Phys. Rev. Lett. **127**, 151102 (2021), arXiv:2107.01298 [gr-qc].
[74] Barry Wardell, Adam Pound, Niels Warburton, Jeremy Miller, Leanne Durkan, and Alexandre Le Tiec, "Gravitational Waveforms for Compact Binaries from Second-Order Self-Force Theory," Phys. Rev. Lett. **130**, 241402 (2023), arXiv:2112.12265 [gr-qc].
[75] A. Buonanno and T. Damour, "Effective one-body approach to general relativistic two-body dynamics," Phys. Rev. D **59**, 084006 (1999), arXiv:gr-qc/9811091.
[76] Alessandra Buonanno and Thibault Damour, "Transition from inspiral to plunge in binary black hole coalescences," Phys. Rev. D **62**, 064015 (2000), arXiv:gr-qc/0001013.
[77] Thibault Damour, Piotr Jaranowski, and Gerhard Schaefer, "On the determination of the last stable orbit for circular general relativistic binaries at the third post-Newtonian approximation," Phys. Rev. D **62**, 084011 (2000), arXiv:gr-qc/0005034.
[78] Thibault Damour, "Coalescence of two spinning black holes: an effective one-body approach," Phys. Rev. D **64**, 124013 (2001), arXiv:gr-qc/0103018.
[79] Alessandra Buonanno, Yanbei Chen, and Thibault Damour, "Transition from inspiral to plunge in precessing binaries of spinning black holes," Phys. Rev. D **74**, 104005 (2006), arXiv:gr-qc/0508067.
[80] Alessandra Buonanno, Gregory B. Cook, and Frans Pretorius, "Inspiral, merger and ring-down of equal-mass black-hole binaries," Phys. Rev. D **75**, 124018 (2007), arXiv:gr-qc/0610122.
[81] Alessandra Buonanno, Yi Pan, John G. Baker, Joan Centrella, Bernard J. Kelly, Sean T. McWilliams, and James R. van Meter, "Toward faithful templates for non-spinning binary black holes using the effective-one-body approach," Phys. Rev. D **76**, 104049 (2007), arXiv:0706.3732 [gr-qc].
[82] Thibault Damour and Alessandro Nagar, "Comparing Effective-One-Body gravitational waveforms to accurate numerical data," Phys. Rev. D **77**, 024043 (2008), arXiv:0711.2628 [gr-qc].
[83] Yi Pan, Alessandra Buonanno, Michael Boyle, Luisa T. Buchman, Lawrence E. Kidder, Harald P. Pfeiffer, and Mark A. Scheel, "Inspiral-merger-ringdown multipolar waveforms of nonspinning black-hole binaries using the effective-one-body formalism," Phys. Rev. D **84**, 124052 (2011), arXiv:1106.1021 [gr-qc].
[84] Thibault Damour, Alessandro Nagar, and Sebastiano Bernuzzi, "Improved effective-one-body description of coalescing nonspinning black-hole binaries and its numerical-relativity completion," Phys. Rev. D **87**, 084035 (2013), arXiv:1212.4357 [gr-qc].
[85] Yi Pan, Alessandra Buonanno, Andrea Taracchini, Lawrence E. Kidder, Abdul H. Mroué, Harald P. Pfeiffer, Mark A. Scheel, and Béla Szilágyi, "Inspiral-merger-ringdown waveforms of spinning, precessing black-hole binaries in the effective-one-body formalism," Phys. Rev. D **89**, 084006 (2014), arXiv:1307.6232 [gr-qc].
[86] Andrea Taracchini *et al.*, "Effective-one-body model for black-hole binaries with generic mass ratios and spins," Phys. Rev. D **89**, 061502 (2014), arXiv:1311.2544 [gr-qc].
[87] Alejandro Bohé *et al.*, "Improved effective-one-body model of spinning, nonprecessing binary black holes for the era of gravitational-wave astrophysics with advanced detectors," Phys. Rev. D **95**, 044028 (2017), arXiv:1611.03703 [gr-qc].
[88] Stanislav Babak, Andrea Taracchini, and Alessandra Buonanno, "Validating the effective-one-body model of spinning, precessing binary black holes against numerical relativity," Phys. Rev. D **95**, 024010 (2017), arXiv:1607.05661 [gr-qc].
[89] Alessandro Nagar *et al.*, "Time-domain effective-one-body gravitational waveforms for coalescing compact binaries with nonprecessing spins, tides and self-spin effects," Phys. Rev. D **98**, 104052 (2018), arXiv:1806.01772 [gr-qc].

[90] Serguei Ossokine *et al.*, "Multipolar Effective-One-Body Waveforms for Precessing Binary Black Holes: Construction and Validation," Phys. Rev. D **102**, 044055 (2020), arXiv:2004.09442 [gr-qc].

[91] Rossella Gamba, Sarp Akçay, Sebastiano Bernuzzi, and Jake Williams, "Effective-one-body waveforms for precessing coalescing compact binaries with post-Newtonian twist," Phys. Rev. D **106**, 024020 (2022), arXiv:2111.03675 [gr-qc].

[92] Alessandro Nagar, Piero Rettegno, Rossella Gamba, Simone Albanesi, Angelica Albertini, and Sebastiano Bernuzzi, "Analytic systematics in next generation of effective-one-body gravitational waveform models for future observations," Phys. Rev. D **108**, 124018 (2023), arXiv:2304.09662 [gr-qc].

[93] Lorenzo Pompili *et al.*, "Laying the foundation of the effective-one-body waveform models SEOBNRv5: Improved accuracy and efficiency for spinning nonprecessing binary black holes," Phys. Rev. D **108**, 124035 (2023), arXiv:2303.18039 [gr-qc].

[94] Antoni Ramos-Buades, Alessandra Buonanno, Héctor Estellés, Mohammed Khalil, Deyan P. Mihaylov, Serguei Ossokine, Lorenzo Pompili, and Mahlet Shiferaw, "Next generation of accurate and efficient multipolar precessing-spin effective-one-body waveforms for binary black holes," Phys. Rev. D **108**, 124037 (2023), arXiv:2303.18046 [gr-qc].

[95] The LVK Collaboration also utilizes phenomenological frequency- and time-domain waveform models, which are built by combining PN, EOB, and NR results [210–212]. Additionally, it employs waveforms directly interpolated from NR simulations [194, 213], where available.

[96] Maarten van de Meent, Alessandra Buonanno, Deyan P. Mihaylov, Serguei Ossokine, Lorenzo Pompili, Niels Warburton, Adam Pound, Barry Wardell, Leanne Durkan, and Jeremy Miller, "Enhancing the SEOBNRv5 effective-one-body waveform model with second-order gravitational self-force fluxes," Phys. Rev. D **108**, 124038 (2023), arXiv:2303.18026 [gr-qc].

[97] Thibault Damour, "Gravitational scattering, post-Minkowskian approximation and Effective One-Body theory," Phys. Rev. **D94**, 104015 (2016), arXiv:1609.00354 [gr-qc].

[98] Clifford Cheung, Ira Z. Rothstein, and Mikhail P. Solon, "From Scattering Amplitudes to Classical Potentials in the Post-Minkowskian Expansion," Phys. Rev. Lett. **121**, 251101 (2018), arXiv:1808.02489 [hep-th].

[99] Zvi Bern, Clifford Cheung, Radu Roiban, Chia-Hsien Shen, Mikhail P. Solon, and Mao Zeng, "Scattering Amplitudes and the Conservative Hamiltonian for Binary Systems at Third Post-Minkowskian Order," Phys. Rev. Lett. **122**, 201603 (2019), arXiv:1901.04424 [hep-th].

[100] Zvi Bern, Dimitrios Kosmopoulos, Andrés Luna, Radu Roiban, and Fei Teng, "Binary Dynamics through the Fifth Power of Spin at O(G2)," Phys. Rev. Lett. **130**, 201402 (2023), arXiv:2203.06202 [hep-th].

[101] David A. Kosower, Ben Maybee, and Donal O'Connell, "Amplitudes, Observables, and Classical Scattering," JHEP **02**, 137 (2019), arXiv:1811.10950 [hep-th].

[102] N.E. J. Bjerrum-Bohr, Poul H. Damgaard, Guido Festuccia, Ludovic Planté, and Pierre Vanhove, "General Relativity from Scattering Amplitudes," Phys. Rev. Lett. **121**, 171601 (2018), arXiv:1806.04920 [hep-th].

[103] Andrea Cristofoli, N. E. J. Bjerrum-Bohr, Poul H. Damgaard, and Pierre Vanhove, "Post-Minkowskian Hamiltonians in general relativity," Phys. Rev. **D100**, 084040 (2019), arXiv:1906.01579 [hep-th].

[104] Poul H. Damgaard, Kays Haddad, and Andreas Helset, "Heavy Black Hole Effective Theory," JHEP **11**, 070 (2019), arXiv:1908.10308 [hep-ph].

[105] Andreas Brandhuber, Gang Chen, Gabriele Travaglini, and Congkao Wen, "Classical gravitational scattering from a gauge-invariant double copy," JHEP **10**, 118 (2021), arXiv:2108.04216 [hep-th].

[106] Justin Vines, "Scattering of two spinning black holes in post-Minkowskian gravity, to all orders in spin, and effective-one-body mappings," Class. Quant. Grav. **35**, 084002 (2018), arXiv:1709.06016 [gr-qc].

[107] Kälin, Gregor and Porto, Rafael A., "Post-Minkowskian Effective Field Theory for Conservative Binary Dynamics," JHEP **11**, 106 (2020), arXiv:2006.01184 [hep-th].

[108] Kälin, Gregor and Liu, Zhengwen and Porto, Rafael A., "Conservative Dynamics of Binary Systems to Third Post-Minkowskian Order from the Effective Field Theory Approach," Phys. Rev. Lett. **125**, 261103 (2020), arXiv:2007.04977 [hep-th].

[109] Gustav Mogull, Jan Plefka, and Jan Steinhoff, "Classical black hole scattering from a worldline quantum field theory," JHEP **02**, 048 (2021), arXiv:2010.02865 [hep-th].

[110] Gustav Uhre Jakobsen, Gustav Mogull, Jan Plefka, and Jan Steinhoff, "SUSY in the sky with gravitons," JHEP **01**, 027 (2022), arXiv:2109.04465 [hep-th].

[111] Gustav Uhre Jakobsen, Gustav Mogull, Jan Plefka, and Benjamin Sauer, "All things retarded: radiation-reaction in worldline quantum field theory," JHEP **10**, 128 (2022), arXiv:2207.00569 [hep-th].

[112] Mohammed Khalil, Alessandra Buonanno, Jan Steinhoff, and Justin Vines, "Energetics and scattering of gravitational two-body systems at fourth post-Minkowskian order," Phys. Rev. D **106**, 024042 (2022), arXiv:2204.05047 [gr-qc].

[113] Zvi Bern, Julio Parra-Martinez, Radu Roiban, Michael S. Ruf, Chia-Hsien Shen, Mikhail P. Solon, and Mao Zeng, "Scattering Amplitudes and Conservative Binary Dynamics at $\mathcal{O}(G^4)$," Phys. Rev. Lett. **126**, 171601 (2021), arXiv:2101.07254 [hep-th].

[114] Zvi Bern, Julio Parra-Martinez, Radu Roiban, Michael S. Ruf, Chia-Hsien Shen, Mikhail P. Solon, and Mao Zeng, "Scattering Amplitudes, the Tail Effect, and Conservative Binary Dynamics at O(G4)," Phys. Rev. Lett. **128**, 161103 (2022), arXiv:2112.10750 [hep-th].

[115] Poul H. Damgaard, Elias Roos Hansen, Ludovic Planté, and Pierre Vanhove, "Classical observables from the exponential representation of the gravitational S-matrix," JHEP **09**, 183 (2023), arXiv:2307.04746 [hep-th].

[116] Christoph Dlapa, Gregor Kälin, Zhengwen Liu, and Rafael A. Porto, "Conservative Dynamics of Binary Systems at Fourth Post-Minkowskian Order in the Large-Eccentricity Expansion," Phys. Rev. Lett. **128**, 161104 (2022), arXiv:2112.11296 [hep-th].

[117] Christoph Dlapa, Gregor Kälin, Zhengwen Liu, and Rafael A. Porto, "Bootstrapping the relativistic two-body problem," JHEP **08**, 109 (2023), arXiv:2304.01275 [hep-th].

[118] Gustav Uhre Jakobsen, Gustav Mogull, Jan Plefka, Benjamin Sauer, and Yingxuan Xu, "Conservative

Scattering of Spinning Black Holes at Fourth Post-Minkowskian Order," Phys. Rev. Lett. **131**, 151401 (2023), arXiv:2306.01714 [hep-th].

[119] Gustav Uhre Jakobsen, Gustav Mogull, Jan Plefka, and Benjamin Sauer, "Tidal effects and renormalization at fourth post-Minkowskian order," Phys. Rev. D **109**, L041504 (2024), arXiv:2312.00719 [hep-th].

[120] Julio Parra-Martinez, Michael S. Ruf, and Mao Zeng, "Extremal black hole scattering at $\mathcal{O}(G^3)$: graviton dominance, eikonal exponentiation, and differential equations," JHEP **11**, 023 (2020), arXiv:2005.04236 [hep-th].

[121] Stefan Weinzierl, "Feynman Integrals," (2022) arXiv:2201.03593 [hep-th].

[122] Samuel Abreu, Ruth Britto, and Claude Duhr, "The SAGEX review on scattering amplitudes Chapter 3: Mathematical structures in Feynman integrals," J. Phys. A **55**, 443004 (2022), arXiv:2203.13014 [hep-th].

[123] Johannes Blümlein and Carsten Schneider, "Chapter 4: Multi-loop Feynman integrals," J. Phys. A **55**, 443005 (2022), arXiv:2203.13015 [hep-th].

[124] Hjalte Frellesvig, Roger Morales, and Matthias Wilhelm, "Calabi-Yau Meets Gravity: A Calabi-Yau Threefold at Fifth Post-Minkowskian Order," Phys. Rev. Lett. **132**, 201602 (2024), arXiv:2312.11371 [hep-th].

[125] Hjalte Frellesvig, Roger Morales, and Matthias Wilhelm, "Classifying post-Minkowskian geometries for gravitational waves via loop-by-loop Baikov," (2024), arXiv:2405.17255 [hep-th].

[126] Albrecht Klemm, Christoph Nega, Benjamin Sauer, and Jan Plefka, "CY in the Sky," (2024), arXiv:2401.07899 [hep-th].

[127] Zvi Bern, Lance J. Dixon, David C. Dunbar, and David A. Kosower, "Fusing gauge theory tree amplitudes into loop amplitudes," Nucl. Phys. **B435**, 59–101 (1995), arXiv:hep-ph/9409265 [hep-ph].

[128] Zvi Bern and Yu-tin Huang, "Basics of Generalized Unitarity," J. Phys. A **44**, 454003 (2011), arXiv:1103.1869 [hep-th].

[129] Zvi Bern, John Joseph M. Carrasco, and Henrik Johansson, "Perturbative Quantum Gravity as a Double Copy of Gauge Theory," Phys. Rev. Lett. **105**, 061602 (2010), arXiv:1004.0476 [hep-th].

[130] Zvi Bern, John Joseph Carrasco, Marco Chiodaroli, Henrik Johansson, and Radu Roiban, "The Duality Between Color and Kinematics and its Applications," (2019), arXiv:1909.01358 [hep-th].

[131] Zvi Bern, John Joseph Carrasco, Marco Chiodaroli, Henrik Johansson, and Radu Roiban, "The SAGEX review on scattering amplitudes Chapter 2: An invitation to color-kinematics duality and the double copy," J. Phys. A **55**, 443003 (2022), arXiv:2203.13013 [hep-th].

[132] Tim Adamo, John Joseph M. Carrasco, Mariana Carrillo-González, Marco Chiodaroli, Henriette Elvang, Henrik Johansson, Donal O'Connell, Radu Roiban, and Oliver Schlotterer, "Snowmass White Paper: the Double Copy and its Applications," in *2022 Snowmass Summer Study* (2022) arXiv:2204.06547 [hep-th].

[133] Ming-Zhi Chung, Yu-Tin Huang, Jung-Wook Kim, and Sangmin Lee, "The simplest massive S-matrix: from minimal coupling to Black Holes," JHEP **04**, 156 (2019), arXiv:1812.08752 [hep-th].

[134] Nima Arkani-Hamed, Yu-tin Huang, and Donal O'Connell, "Kerr black holes as elementary particles," JHEP **01**, 046 (2020), arXiv:1906.10100 [hep-th].

[135] Zvi Bern, Andres Luna, Radu Roiban, Chia-Hsien Shen, and Mao Zeng, "Spinning black hole binary dynamics, scattering amplitudes, and effective field theory," Phys. Rev. D **104**, 065014 (2021), arXiv:2005.03071 [hep-th].

[136] Yilber Fabian Bautista, Alfredo Guevara, Chris Kavanagh, and Justin Vines, "Scattering in black hole backgrounds and higher-spin amplitudes. Part I," JHEP **03**, 136 (2023), arXiv:2107.10179 [hep-th].

[137] Yilber Fabian Bautista, Alfredo Guevara, Chris Kavanagh, and Justin Vines, "Scattering in black hole backgrounds and higher-spin amplitudes. Part II," JHEP **05**, 211 (2023), arXiv:2212.07965 [hep-th].

[138] Marco Chiodaroli, Henrik Johansson, and Paolo Pichini, "Compton black-hole scattering for s $\leq$ 5/2," JHEP **02**, 156 (2022), arXiv:2107.14779 [hep-th].

[139] Rafael Aoude, Kays Haddad, and Andreas Helset, "Classical gravitational scattering amplitude at O(G2S1∞S2∞)," Phys. Rev. D **108**, 024050 (2023), arXiv:2304.13740 [hep-th].

[140] Lucile Cangemi, Marco Chiodaroli, Henrik Johansson, Alexander Ochirov, Paolo Pichini, and Evgeny Skvortsov, "From higher-spin gauge interactions to Compton amplitudes for root-Kerr," (2023), arXiv:2311.14668 [hep-th].

[141] Mohammed Khalil, Alessandra Buonanno, Hector Estelles, Deyan P. Mihaylov, Serguei Ossokine, Lorenzo Pompili, and Antoni Ramos-Buades, "Theoretical groundwork supporting the precessing-spin two-body dynamics of the effective-one-body waveform models SEOBNRv5," Phys. Rev. D **108**, 124036 (2023), arXiv:2303.18143 [gr-qc].

[142] Alessandra Buonanno, Gustav Uhre Jakobsen, and Gustav Mogull, "Post-Minkowskian Theory Meets the Spinning Effective-One-Body Approach for Two-Body Scattering," (2024), arXiv:2402.12342 [gr-qc].

[143] Alfredo Guevara, Alexander Ochirov, and Justin Vines, "Scattering of Spinning Black Holes from Exponentiated Soft Factors," JHEP **09**, 056 (2019), arXiv:1812.06895 [hep-th].

[144] Dimitrios Kosmopoulos and Andres Luna, "Quadratic-in-spin Hamiltonian at $\mathcal{O}(\mathrm{G}^2)$ from scattering amplitudes," JHEP **07**, 037 (2021), arXiv:2102.10137 [hep-th].

[145] Wei-Ming Chen, Ming-Zhi Chung, Yu-tin Huang, and Jung-Wook Kim, "The 2PM Hamiltonian for binary Kerr to quartic in spin," JHEP **08**, 148 (2022), arXiv:2111.13639 [hep-th].

[146] Gustav Uhre Jakobsen and Gustav Mogull, "Conservative and Radiative Dynamics of Spinning Bodies at Third Post-Minkowskian Order Using Worldline Quantum Field Theory," Phys. Rev. Lett. **128**, 141102 (2022), arXiv:2201.07778 [hep-th].

[147] Gustav Uhre Jakobsen and Gustav Mogull, "Linear response, Hamiltonian, and radiative spinning two-body dynamics," Phys. Rev. D **107**, 044033 (2023), arXiv:2210.06451 [hep-th].

[148] Fernando Febres Cordero, Manfred Kraus, Guanda Lin, Michael S. Ruf, and Mao Zeng, "Conservative Binary Dynamics with a Spinning Black Hole at O(G3) from Scattering Amplitudes," Phys. Rev. Lett. **130**, 021601 (2023), arXiv:2205.07357 [hep-th].

[149] We plan to update our `SEOBNR-PM` model in the near future to include the recent findings in Ref. [197], which

allow to derive the local-in-time EOB Hamiltonian for bound orbits at 4PM.

[150] Deyan P. Mihaylov, Serguei Ossokine, Alessandra Buonanno, Hector Estelles, Lorenzo Pompili, Michael Pürrer, and Antoni Ramos-Buades, "pySEOBNR: a software package for the next generation of effective-one-body multipolar waveform models," (2023), arXiv:2303.18203 [gr-qc].

[151] Thibault Damour, Bala R. Iyer, and Alessandro Nagar, "Improved resummation of post-Newtonian multipolar waveforms from circularized compact binaries," Phys. Rev. D **79**, 064004 (2009), arXiv:0811.2069 [gr-qc].

[152] Thibault Damour and Alessandro Nagar, "Faithful effective-one-body waveforms of small-mass-ratio coalescing black-hole binaries," Phys. Rev. D **76**, 064028 (2007), arXiv:0705.2519 [gr-qc].

[153] Yi Pan, Alessandra Buonanno, Ryuichi Fujita, Etienne Racine, and Hideyuki Tagoshi, "Post-Newtonian factorized multipolar waveforms for spinning, non-precessing black-hole binaries," Phys. Rev. D **83**, 064003 (2011), [Erratum: Phys.Rev.D 87, 109901 (2013)], arXiv:1006.0431 [gr-qc].

[154] Thibault Damour, Bala R. Iyer, Piotr Jaranowski, and B. S. Sathyaprakash, "Gravitational waves from black hole binary inspiral and merger: The Span of third post-Newtonian effective one-body templates," Phys. Rev. D **67**, 064028 (2003), arXiv:gr-qc/0211041.

[155] Thibault Damour and Alessandro Nagar, "A new analytic representation of the ringdown waveform of coalescing spinning black hole binaries," Phys. Rev. D **90**, 024054 (2014), arXiv:1406.0401 [gr-qc].

[156] Roberto Cotesta, Alessandra Buonanno, Alejandro Bohé, Andrea Taracchini, Ian Hinder, and Serguei Ossokine, "Enriching the Symphony of Gravitational Waves from Binary Black Holes by Tuning Higher Harmonics," Phys. Rev. D **98**, 084028 (2018), arXiv:1803.10701 [gr-qc].

[157] Mathias Driesse, Gustav Uhre Jakobsen, Gustav Mogull, Jan Plefka, Benjamin Sauer, and Johann Usovitsch, "Conservative Black Hole Scattering at Fifth Post-Minkowskian and First Self-Force Order," (2024), arXiv:2403.07781 [hep-th].

[158] Thibault Damour, "High-energy gravitational scattering and the general relativistic two-body problem," Phys. Rev. **D97**, 044038 (2018), arXiv:1710.10599 [gr-qc].

[159] Andrea Antonelli, Alessandra Buonanno, Jan Steinhoff, Maarten van de Meent, and Justin Vines, "Energetics of two-body Hamiltonians in post-Minkowskian gravity," Phys. Rev. **D99**, 104004 (2019), arXiv:1901.07102 [gr-qc].

[160] Andrea Antonelli, Chris Kavanagh, Mohammed Khalil, Jan Steinhoff, and Justin Vines, "Gravitational spin-orbit coupling through third-subleading post-Newtonian order: from first-order self-force to arbitrary mass ratios," Phys. Rev. Lett. **125**, 011103 (2020), arXiv:2003.11391 [gr-qc].

[161] Manoj K. Mandal, Pierpaolo Mastrolia, Raj Patil, and Jan Steinhoff, "Gravitational spin-orbit Hamiltonian at NNNLO in the post-Newtonian framework," JHEP **03**, 130 (2023), arXiv:2209.00611 [hep-th].

[162] Jung-Wook Kim, Michèle Levi, and Zhewei Yin, "N^3LO spin-orbit interaction via the EFT of spinning gravitating objects," JHEP **05**, 184 (2023), arXiv:2208.14949 [hep-th].

[163] Michele Levi and Jan Steinhoff, "Leading order finite size effects with spins for inspiralling compact binaries," JHEP **06**, 059 (2015), arXiv:1410.2601 [gr-qc].

[164] We thank Mohammed Khalil for providing us with suitable PN Hamiltonians to compare with.

[165] As a spin-dependent bound-orbit correction would only arise at 5.5PN order, we choose not to include it.

[166] Serguei Ossokine, Tim Dietrich, Evan Foley, Reza Katebi, and Geoffrey Lovelace, "Assessing the Energetics of Spinning Binary Black Hole Systems," Phys. Rev. D **98**, 104057 (2018), arXiv:1712.06533 [gr-qc].

[167] Stefan Behnel, Robert Bradshaw, Craig Citro, Lisandro Dalcin, Dag Sverre Seljebotn, and Kurt Smith, "Cython: The Best of Both Worlds," Comput. Sci. Eng. **13**, 31–39 (2011).

[168] Thibault Damour, Alessandro Nagar, Denis Pollney, and Christian Reisswig, "Energy versus Angular Momentum in Black Hole Binaries," Phys. Rev. Lett. **108**, 131101 (2012), arXiv:1110.2938 [gr-qc].

[169] Alexandre Le Tiec, Enrico Barausse, and Alessandra Buonanno, "Gravitational Self-Force Correction to the Binding Energy of Compact Binary Systems," Phys. Rev. Lett. **108**, 131103 (2012), arXiv:1111.5609 [gr-qc].

[170] Alessandro Nagar, Thibault Damour, Christian Reisswig, and Denis Pollney, "Energetics and phasing of nonprecessing spinning coalescing black hole binaries," Phys. Rev. D **93**, 044046 (2016), arXiv:1506.08457 [gr-qc].

[171] Alexandre Le Tiec, Abdul H. Mroue, Leor Barack, Alessandra Buonanno, Harald P. Pfeiffer, Norichika Sago, and Andrea Taracchini, "Periastron Advance in Black Hole Binaries," Phys. Rev. Lett. **107**, 141101 (2011), arXiv:1106.3278 [gr-qc].

[172] Tanja Hinderer *et al.*, "Periastron advance in spinning black hole binaries: comparing effective-one-body and Numerical Relativity," Phys. Rev. D **88**, 084005 (2013), arXiv:1309.0544 [gr-qc].

[173] Tim Dietrich, Sebastiano Bernuzzi, Maximiliano Ujevic, and Wolfgang Tichy, "Gravitational waves and mass ejecta from binary neutron star mergers: Effect of the stars' rotation," Phys. Rev. D **95**, 044045 (2017), arXiv:1611.07367 [gr-qc].

[174] James M. Bardeen, William H. Press, and Saul A Teukolsky, "Rotating black holes: Locally nonrotating frames, energy extraction, and scalar synchrotron radiation," Astrophys. J. **178**, 347 (1972).

[175] Xisco Jiménez-Forteza, David Keitel, Sascha Husa, Mark Hannam, Sebastian Khan, and Michael Pürrer, "Hierarchical data-driven approach to fitting numerical relativity data for nonprecessing binary black holes with an application to final spin and radiated energy," Phys. Rev. D **95**, 064024 (2017), arXiv:1611.00332 [gr-qc].

[176] Fabian Hofmann, Enrico Barausse, and Luciano Rezzolla, "The final spin from binary black holes in quasi-circular orbits," Astrophys. J. Lett. **825**, L19 (2016), arXiv:1605.01938 [gr-qc].

[177] More specifically, the `SEOBNRv5`'s Hamiltonian employs all known 5PN coefficients in the A- and D-potentials (except for the partially known 5PN local part of the A-potential that is fully replaced by the a_6 calibration coefficient), and the 5.5PN terms in the Q-potential. Although the 4.5PN spin-orbit couplings are known, Ref. [93] did not use them (but the 3.5PN), because

the authors showed that having a spin-orbit calibration parameter at 5.5PN (instead of 4.5PN) is not very effective.

[178] B. S. Sathyaprakash and S. V. Dhurandhar, "Choice of filters for the detection of gravitational waves from coalescing binaries," Phys. Rev. D **44**, 3819–3834 (1991).

[179] Lee Samuel Finn and David F. Chernoff, "Observing binary inspiral in gravitational radiation: One interferometer," Phys. Rev. D **47**, 2198–2219 (1993), arXiv:gr-qc/9301003.

[180] Lisa Barsotti, Peter Fritschel, Matthew Evans, and Slawomir Gras (LIGO Collaboration), "Updated advanced ligo sensitivity design curve," `https://dcc.ligo.org/LIGO-T1800044/public` (2018), LIGO Document T1800044-v5.

[181] Gregory Ashton *et al.*, "BILBY: A user-friendly Bayesian inference library for gravitational-wave astronomy," Astrophys. J. Suppl. **241**, 27 (2019), arXiv:1811.02042 [astro-ph.IM].

[182] Michael Boyle *et al.*, "The SXS Collaboration catalog of binary black hole simulations," Class. Quant. Grav. **36**, 195006 (2019), arXiv:1904.04831 [gr-qc].

[183] Abdul H. Mroue *et al.*, "Catalog of 174 Binary Black Hole Simulations for Gravitational Wave Astronomy," Phys. Rev. Lett. **111**, 241104 (2013), arXiv:1304.6077 [gr-qc].

[184] Daniel A. Hemberger, Geoffrey Lovelace, Thomas J. Loredo, Lawrence E. Kidder, Mark A. Scheel, Bela Szilagyi, Nicholas W. Taylor, and Saul A. Teukolsky, "Final spin and radiated energy in numerical simulations of binary black holes with equal masses and equal, aligned or anti-aligned spins," Phys. Rev. **D88**, 064014 (2013), arXiv:1305.5991 [gr-qc].

[185] Mark A. Scheel, Matthew Giesler, Daniel A. Hemberger, Geoffrey Lovelace, Kevin Kuper, Michael Boyle, B. Szilagyi, and Lawrence E. Kidder, "Improved methods for simulating nearly extremal binary black holes," Class. Quant. Grav. **32**, 105009 (2015), arXiv:1412.1803 [gr-qc].

[186] Geoffrey Lovelace *et al.*, "Nearly extremal apparent horizons in simulations of merging black holes," Class. Quant. Grav. **32**, 065007 (2015), arXiv:1411.7297 [gr-qc].

[187] Tony Chu, Heather Fong, Prayush Kumar, Harald P. Pfeiffer, Michael Boyle, Daniel A. Hemberger, Lawrence E. Kidder, Mark A. Scheel, and Bela Szilagyi, "On the accuracy and precision of numerical waveforms: Effect of waveform extraction methodology," Class. Quant. Grav. **33**, 165001 (2016), arXiv:1512.06800 [gr-qc].

[188] Jonathan Blackman, Scott E. Field, Chad R. Galley, Bela Szilagyi, Mark A. Scheel, Manuel Tiglio, and Daniel A. Hemberger, "Fast and Accurate Prediction of Numerical Relativity Waveforms from Binary Black Hole Coalescences Using Surrogate Models," Phys. Rev. Lett. **115**, 121102 (2015), arXiv:1502.07758 [gr-qc].

[189] B. P. Abbott *et al.* (Virgo, LIGO Scientific), "GW151226: Observation of Gravitational Waves from a 22-Solar-Mass Binary Black Hole Coalescence," Phys. Rev. Lett. **116**, 241103 (2016), arXiv:1606.04855 [gr-qc].

[190] B. P. Abbott *et al.* (Virgo, LIGO Scientific), "Directly comparing GW150914 with numerical solutions of Einsteins equations for binary black hole coalescence," Phys. Rev. **D94**, 064035 (2016), arXiv:1606.01262 [gr-qc].

[191] Geoffrey Lovelace *et al.*, "Modeling the source of GW150914 with targeted numerical-relativity simulations," Class. Quant. Grav. **33**, 244002 (2016), arXiv:1607.05377 [gr-qc].

[192] Jonathan Blackman, Scott E. Field, Mark A. Scheel, Chad R. Galley, Daniel A. Hemberger, Patricia Schmidt, and Rory Smith, "A Surrogate Model of Gravitational Waveforms from Numerical Relativity Simulations of Precessing Binary Black Hole Mergers," Phys. Rev. D **95**, 104023 (2017), arXiv:1701.00550 [gr-qc].

[193] Vijay Varma, Scott E. Field, Mark A. Scheel, Jonathan Blackman, Lawrence E. Kidder, and Harald P. Pfeiffer, "Surrogate model of hybridized numerical relativity binary black hole waveforms," Phys. Rev. D **99**, 064045 (2019), arXiv:1812.07865 [gr-qc].

[194] Vijay Varma, Scott E. Field, Mark A. Scheel, Jonathan Blackman, Davide Gerosa, Leo C. Stein, Lawrence E. Kidder, and Harald P. Pfeiffer, "Surrogate models for precessing binary black hole simulations with unequal masses," Phys. Rev. Research. **1**, 033015 (2019), arXiv:1905.09300 [gr-qc].

[195] Jooheon Yoo, Vijay Varma, Matthew Giesler, Mark A. Scheel, Carl-Johan Haster, Harald P. Pfeiffer, Lawrence E. Kidder, and Michael Boyle, "Targeted large mass ratio numerical relativity surrogate waveform model for GW190814," Phys. Rev. D **106**, 044001 (2022), arXiv:2203.10109 [gr-qc].

[196] When using the `SEOBNRv5` model with 4.5PN spin-orbit couplings and calibrate $\Delta t_{\rm NR}$, we find a better agreement than the model with 3.5PN, but `SEOBNR-PM` performs still better.

[197] Christoph Dlapa, Gregor Kälin, Zhengwen Liu, and Rafael A. Porto, "Local-in-time Conservative Binary Dynamics at Fourth Post-Minkowskian Order," (2024), arXiv:2403.04853 [hep-th].

[198] Enrico Herrmann, Julio Parra-Martinez, Michael S. Ruf, and Mao Zeng, "Gravitational Bremsstrahlung from Reverse Unitarity," Phys. Rev. Lett. **126**, 201602 (2021), arXiv:2101.07255 [hep-th].

[199] Enrico Herrmann, Julio Parra-Martinez, Michael S. Ruf, and Mao Zeng, "Radiative classical gravitational observables at $\mathcal{O}(\mathrm{G}^3)$ from scattering amplitudes," JHEP **10**, 148 (2021), arXiv:2104.03957 [hep-th].

[200] Paolo Di Vecchia, Carlo Heissenberg, Rodolfo Russo, and Gabriele Veneziano, "The eikonal approach to gravitational scattering and radiation at $\mathcal{O}(\mathrm{G}^3)$," JHEP **07**, 169 (2021), arXiv:2104.03256 [hep-th].

[201] Carlo Heissenberg, "Infrared divergences and the eikonal exponentiation," Phys. Rev. D **104**, 046016 (2021), arXiv:2105.04594 [hep-th].

[202] N. Emil J. Bjerrum-Bohr, Poul H. Damgaard, Ludovic Planté, and Pierre Vanhove, "The amplitude for classical gravitational scattering at third Post-Minkowskian order," JHEP **08**, 172 (2021), arXiv:2105.05218 [hep-th].

[203] Poul H. Damgaard, Ludovic Plante, and Pierre Vanhove, "On an exponential representation of the gravitational S-matrix," JHEP **11**, 213 (2021), arXiv:2107.12891 [hep-th].

[204] Stavros Mougiakakos, Massimiliano Maria Riva, and Filippo Vernizzi, "Gravitational Bremsstrahlung in the post-Minkowskian effective field theory," Phys. Rev. D

104, 024041 (2021), arXiv:2102.08339 [gr-qc].

[205] Aneesh V. Manohar, Alexander K. Ridgway, and Chia-Hsien Shen, "Radiated Angular Momentum and Dissipative Effects in Classical Scattering," Phys. Rev. Lett. **129**, 121601 (2022), arXiv:2203.04283 [hep-th].

[206] Christoph Dlapa, Gregor Kälin, Zhengwen Liu, Jakob Neef, and Rafael A. Porto, "Radiation Reaction and Gravitational Waves at Fourth Post-Minkowskian Order," Phys. Rev. Lett. **130**, 101401 (2023), arXiv:2210.05541 [hep-th].

[207] Gustav Uhre Jakobsen, Gustav Mogull, Jan Plefka, and Jan Steinhoff, "Classical Gravitational Bremsstrahlung from a Worldline Quantum Field Theory," Phys. Rev. Lett. **126**, 201103 (2021), arXiv:2101.12688 [gr-qc].

[208] Gustav Uhre Jakobsen, Gustav Mogull, Jan Plefka, and Jan Steinhoff, "Gravitational Bremsstrahlung and Hidden Supersymmetry of Spinning Bodies," Phys. Rev. Lett. **128**, 011101 (2022), arXiv:2106.10256 [hep-th].

[209] Gustav Uhre Jakobsen, Gustav Mogull, Jan Plefka, and Benjamin Sauer, "Dissipative Scattering of Spinning Black Holes at Fourth Post-Minkowskian Order," Phys. Rev. Lett. **131**, 241402 (2023), arXiv:2308.11514 [hep-th].

[210] Parameswaran Ajith *et al.*, "Phenomenological template family for black-hole coalescence waveforms," Class. Quant. Grav. **24**, S689–S700 (2007), arXiv:0704.3764 [gr-qc].

[211] Geraint Pratten *et al.*, "Computationally efficient models for the dominant and subdominant harmonic modes of precessing binary black holes," Phys. Rev. D **103**, 104056 (2021), arXiv:2004.06503 [gr-qc].

[212] Héctor Estellés, Marta Colleoni, Cecilio García-Quirós, Sascha Husa, David Keitel, Maite Mateu-Lucena, Maria de Lluc Planas, and Antoni Ramos-Buades, "New twists in compact binary waveform modeling: A fast time-domain model for precession," Phys. Rev. D **105**, 084040 (2022), arXiv:2105.05872 [gr-qc].

[213] Jonathan Blackman, Scott E. Field, Mark A. Scheel, Chad R. Galley, Christian D. Ott, Michael Boyle, Lawrence E. Kidder, Harald P. Pfeiffer, and Béla Szilágyi, "Numerical relativity waveform surrogate model for generically precessing binary black hole mergers," Phys. Rev. D **96**, 024058 (2017), arXiv:1705.07089 [gr-qc].